

Recent results on hadron physics at Belle and Belle II



Makoto Takizawa

Showa Pharmaceutical University

J-PARC Branch, Theory Center, IPNS, KEK

Meson Science Lab. CPR, RIKEN

on behalf of Belle and Belle II collaborations

Outline

- Introduction of Belle experiment
- Introduction of Belle II experiment
- Recent results on hadron physics at Belle

$\Omega(2012)$ related
Spin-parity of $\Xi_c(2970)$

- Recent results on hadron physics at Belle II

Observation of $\Upsilon(10753) \rightarrow \omega\chi_{bJ}(1P)$
Search for $X_b \rightarrow \omega\Upsilon(1S)$

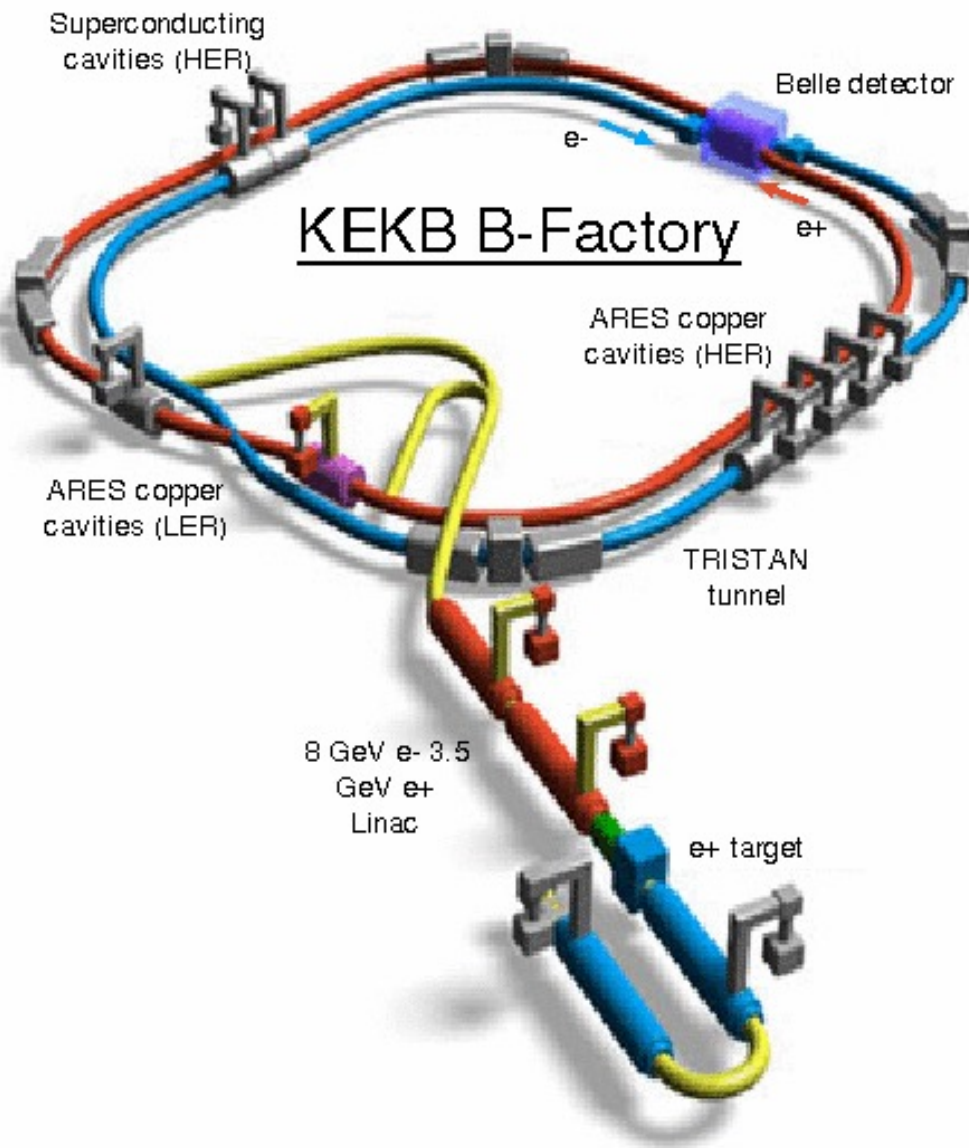
- Summary

Introduction of Belle experiment

Belle experiment is the experiment at KEK B factory with Belle detector dedicated for the CP violation physics of B mesons

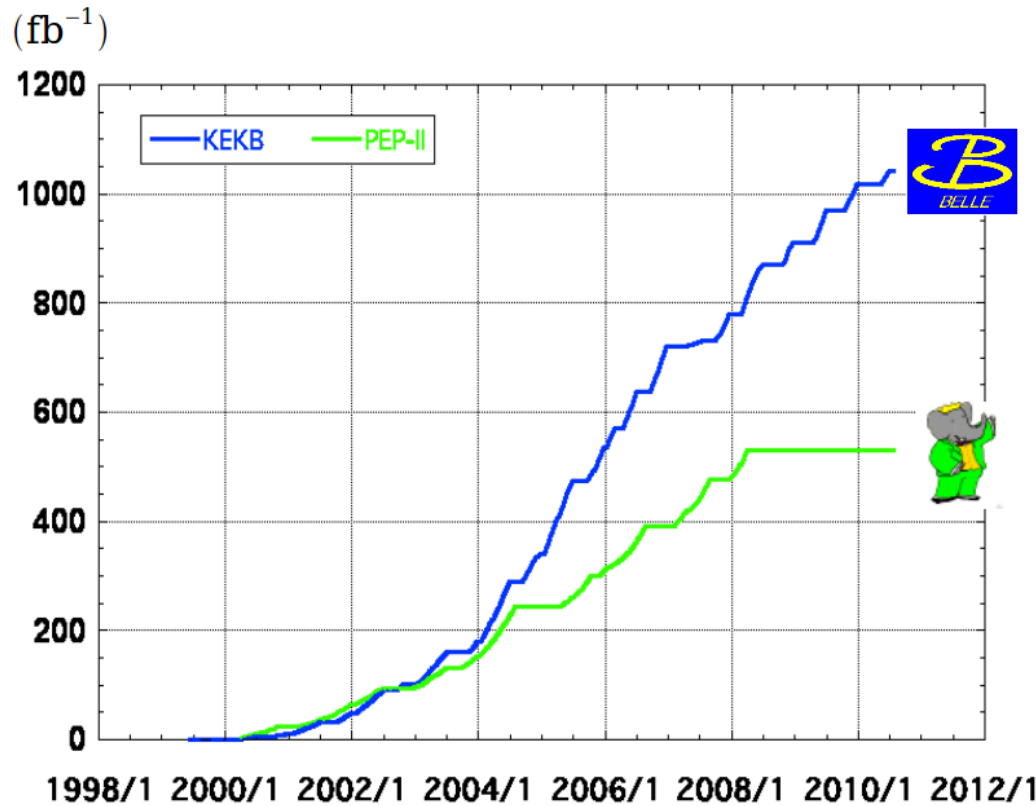
High resolution, multipurpose, good PID, 4π spectrometer

Loose event selection



- $8\text{GeV}(e^-) \times 3.5\text{GeV}(e^+)$
- Peak Luminosity $2.1 \times 10^{34} \text{ cm}^{-2} \text{ s}^{-1}$
- Integrated luminosity 1040 fb^{-1}

Integrated luminosity of B factories



> 1 ab^{-1}

On resonance:

$\Upsilon(5S)$: 121 fb^{-1}

$\Upsilon(4S)$: 711 fb^{-1}

$\Upsilon(3S)$: 3 fb^{-1}

$\Upsilon(2S)$: 25 fb^{-1}

$\Upsilon(1S)$: 6 fb^{-1}

Off reson./scan:

$\sim 100 \text{ fb}^{-1}$

$\sim 550 \text{ fb}^{-1}$

On resonance:

$\Upsilon(4S)$: 433 fb^{-1}

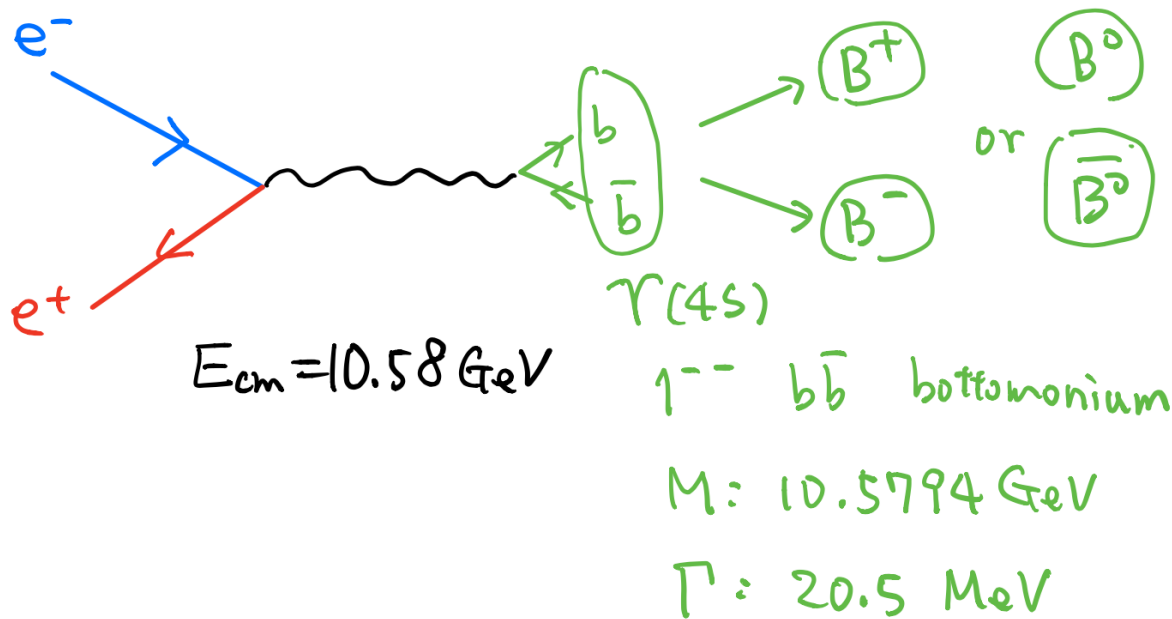
$\Upsilon(3S)$: 30 fb^{-1}

$\Upsilon(2S)$: 14 fb^{-1}

Off resonance:

$\sim 54 \text{ fb}^{-1}$

KEK B factory



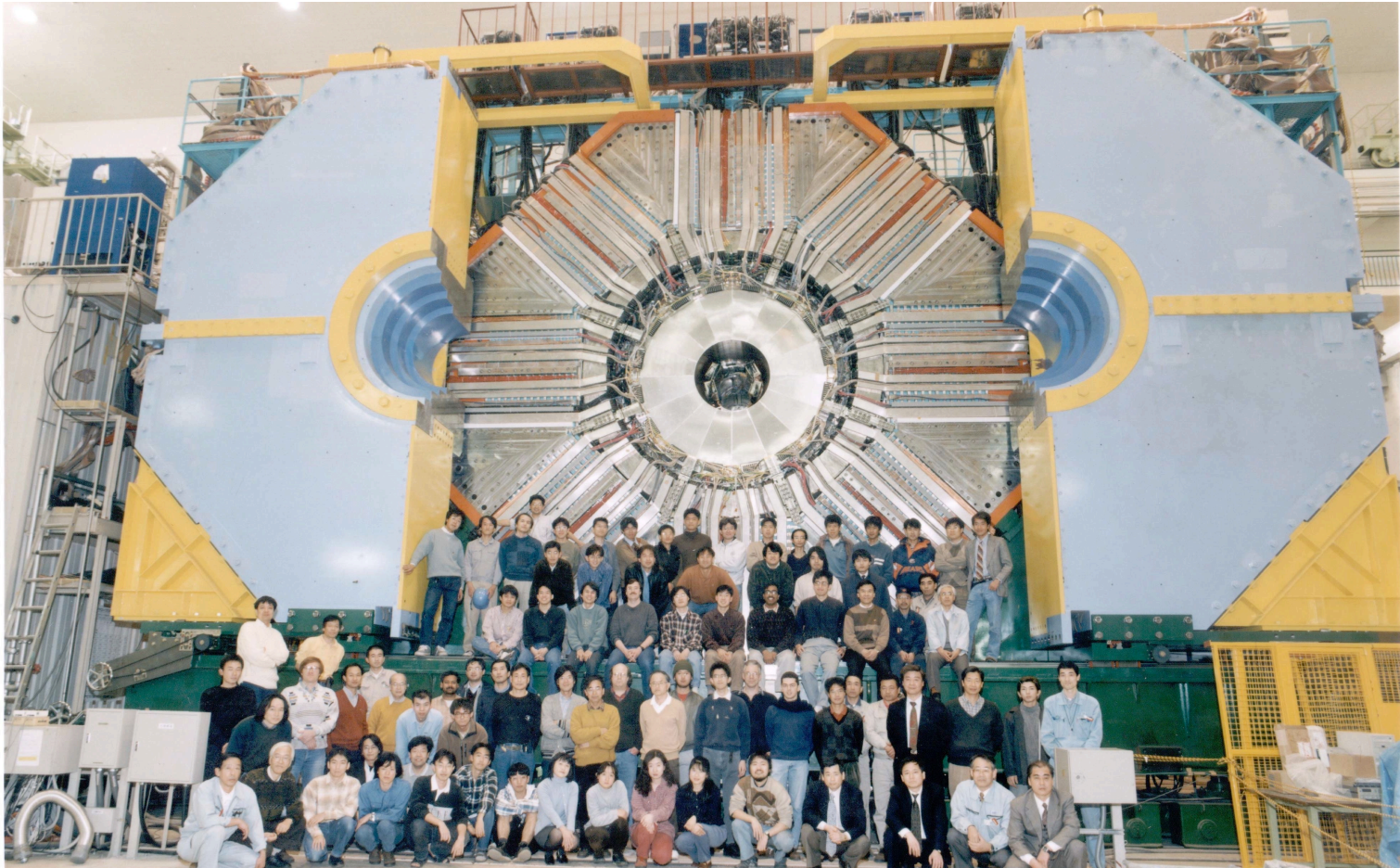
B factories

$\Upsilon(4S) \rightarrow B \bar{B}$
fraction $> 96\%$

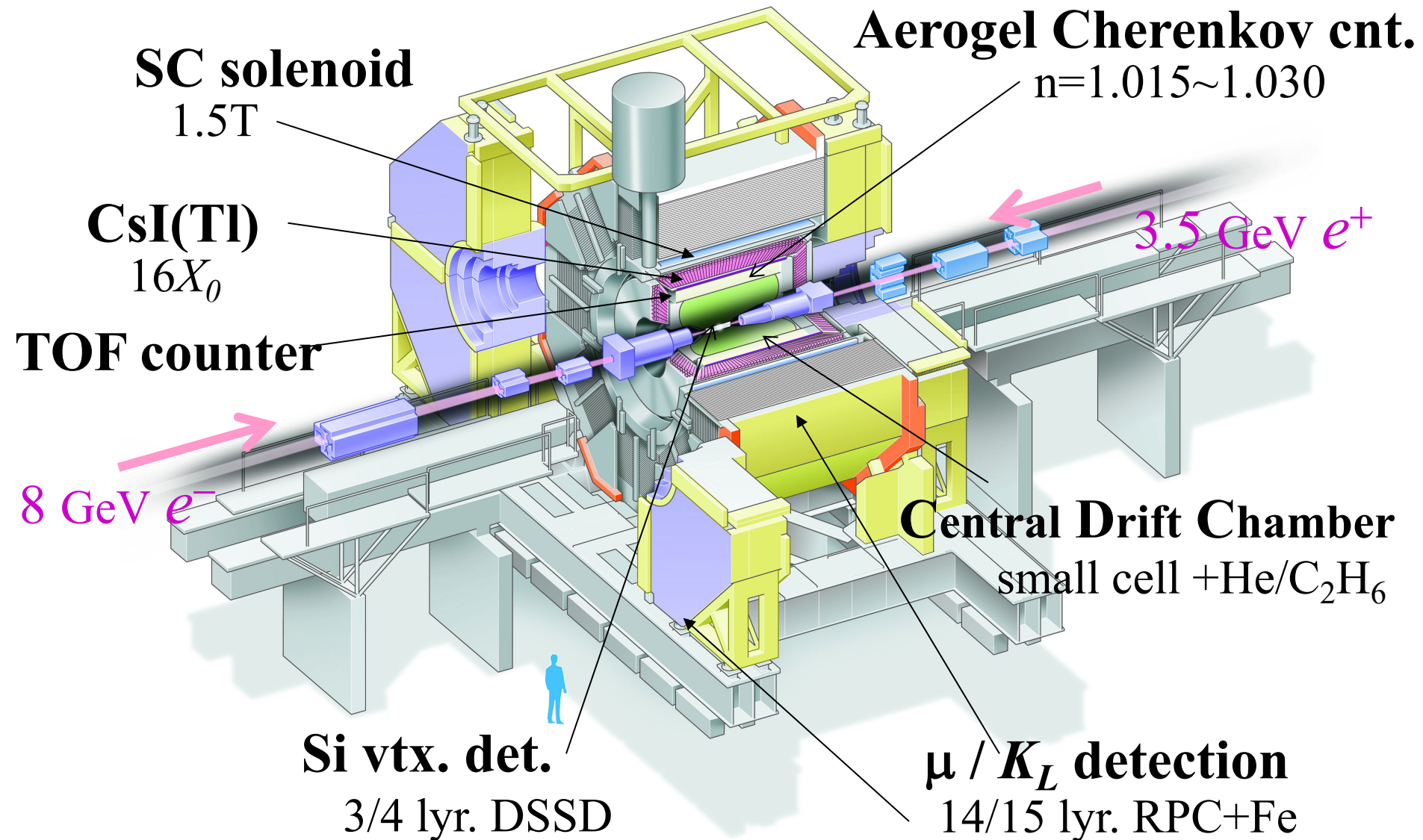
- Reference

Prog. Theor. Exp. Phys. **2013**, 03A001
DOI: 10.1093/ptep/pts102
Achievement of KEKB

Belle detector (already disassembled)



Belle Detector



Data analyses at Belle

Detected particles

- photon
- electron, muon
- Charged hadrons: pion, kaon, proton
- Neutral hadrons: K_L
 $\pi^0 \rightarrow \gamma\gamma$, $\eta \rightarrow \gamma\gamma$, $K_S \rightarrow \pi\pi$, $\Lambda \rightarrow p\pi$

K_L is not used for hadron physics, but for cp violation physics.

Energy, momentum, track, vertex point
Combinations of these data are used for
reconstruction of hadron resonances
For more detail, see PR D 67, 032003 (2003)

Physics runs

Table 1. Summary of the luminosity integrated by Belle, broken down by CM energy.

Resonance	On-peak luminosity (fb^{-1})	Off-peak luminosity (fb^{-1})	Number of resonances
$\Upsilon(1S)$	5.7	1.8	102×10^6
$\Upsilon(2S)$	24.9	1.7	158×10^6
$\Upsilon(3S)$	2.9	0.25	11×10^6
$\Upsilon(4S)$ SVD1	140.0	15.6	$152 \times 10^6 B\bar{B}$
$\Upsilon(4S)$ SVD2	571.0	73.8	$620 \times 10^6 B\bar{B}$
$\Upsilon(5S)$	121.4	1.7	$7.1 \times 10^6 B_s\bar{B}_s$
Scan		27.6	

Reference: J. Brodzicka et. al., PTEP, 2012, 04D001

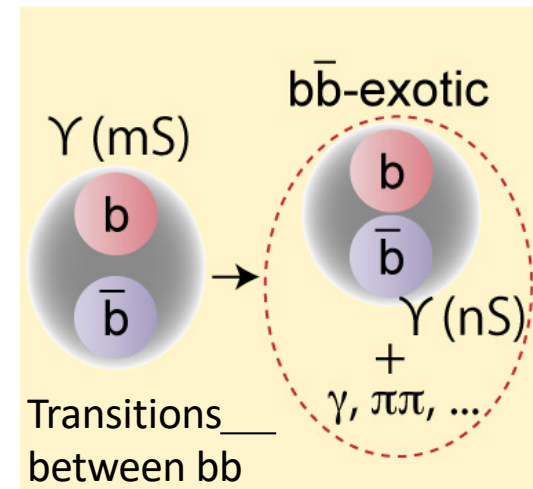
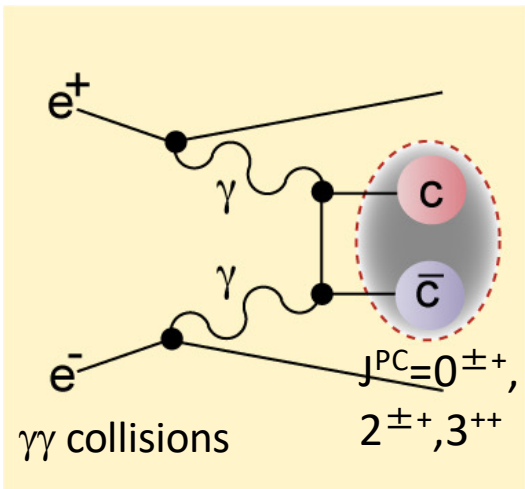
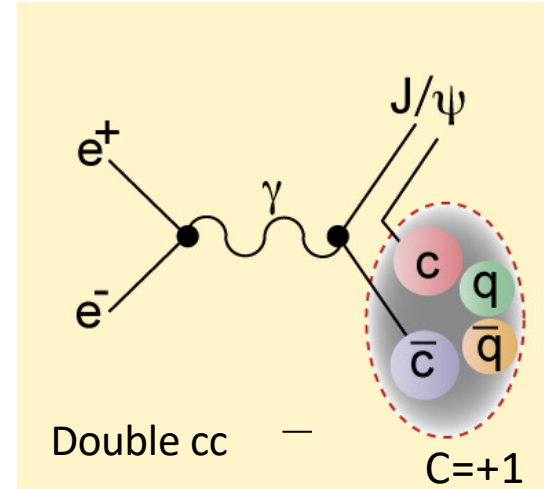
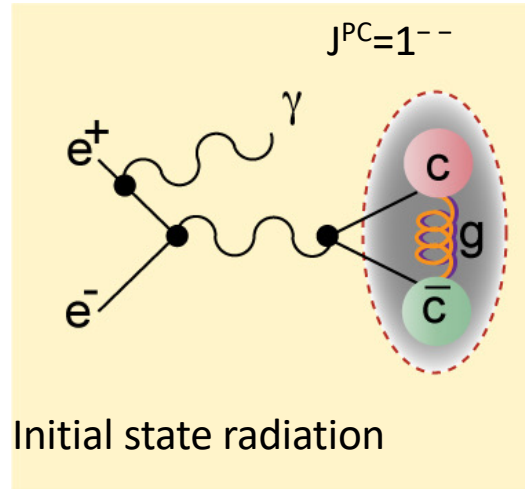
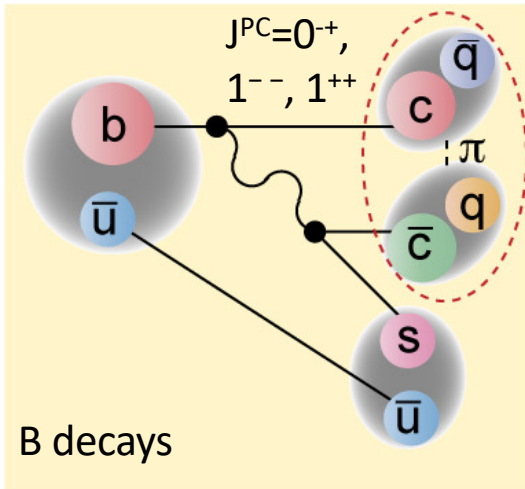
- **Off-resonance data**
60MeV below the resonance peak in order to determine the non- BB^{bar} background
- **Energy scan data**
between $\Upsilon(4S)$ (10.5794GeV) and $\Upsilon(6S)$ (11.019GeV)
- **Tau and Charm factory**
There are many $e^+e^- \rightarrow \bar{u}u, \bar{d}d, \bar{s}s, \bar{c}c, \bar{\tau}\tau$ events created too.

Good points of Belle Experiment for Hadron physics

- Thanks to KEKB high luminosity, we have large data.
- Belle detector is the general purpose, high resolution, nearly 4π spectrometer.
- There are many paths to produce hadrons, such as, B decays, Initial State Radiation, Two photon process, continuum $q\bar{q}$ process, non- $\Upsilon(4S)$ $\Upsilon(1S, 2S, 3S, 5S)$ decays, etc. Process restricts the produced hadron quantum numbers.

Variety of recorded reactions

Miyabayashi-san's slide for EXA2017



Allowed/favored quantum numbers are different depending on production processes.

Good points of Belle Experiment for Hadron physics

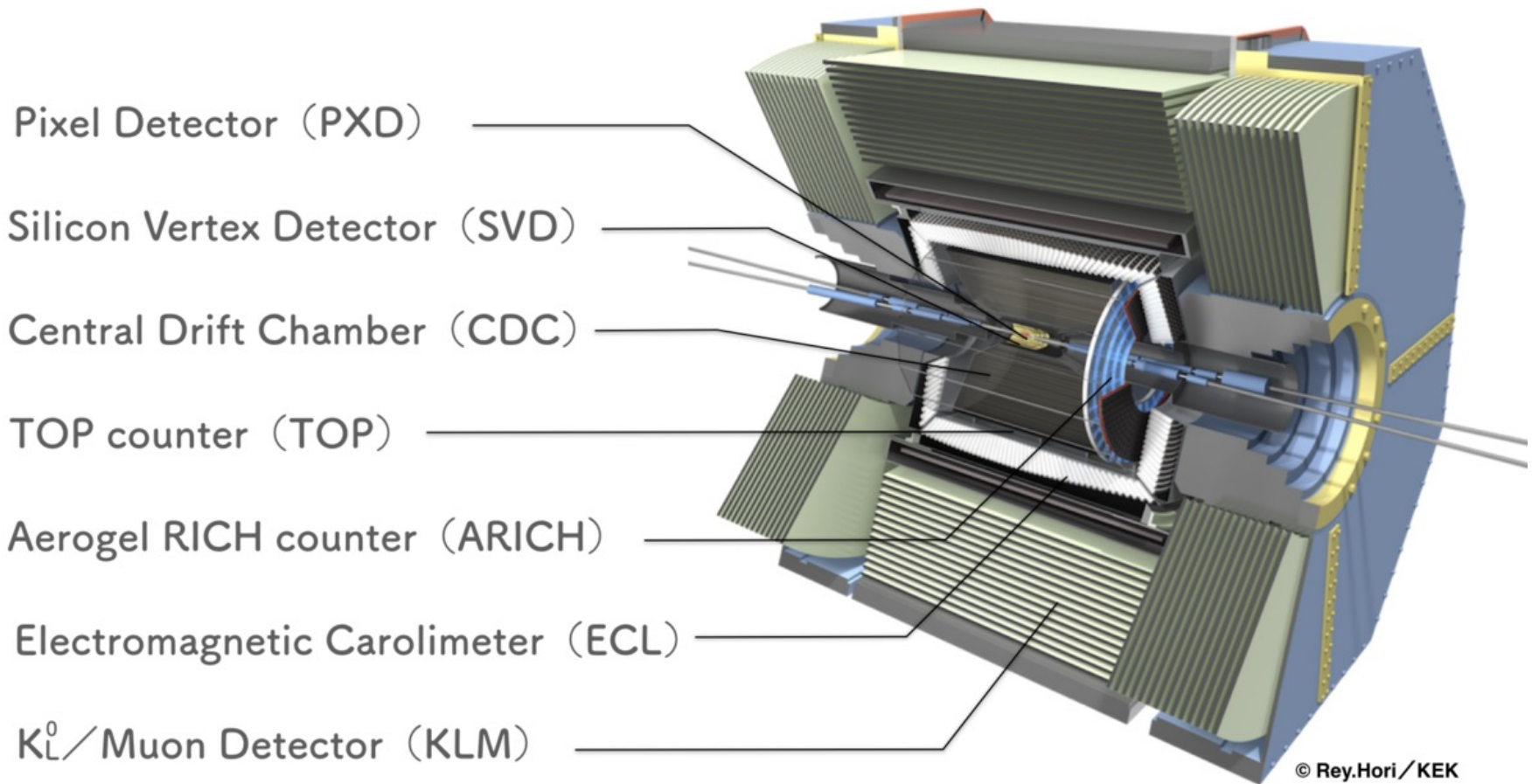
- As for the decays of hadrons, we can measure neutral pion and eta. It helps the study of iso-spin structures of the excited hadrons, such as a charged partner of $X(3872)$ and a charge conjugation minus counterpart of $X(3872)$.
- We can measure radiative decays of hadrons too. The radiative decays give us the information of the hadron structures.

Introduction of Belle II experiment

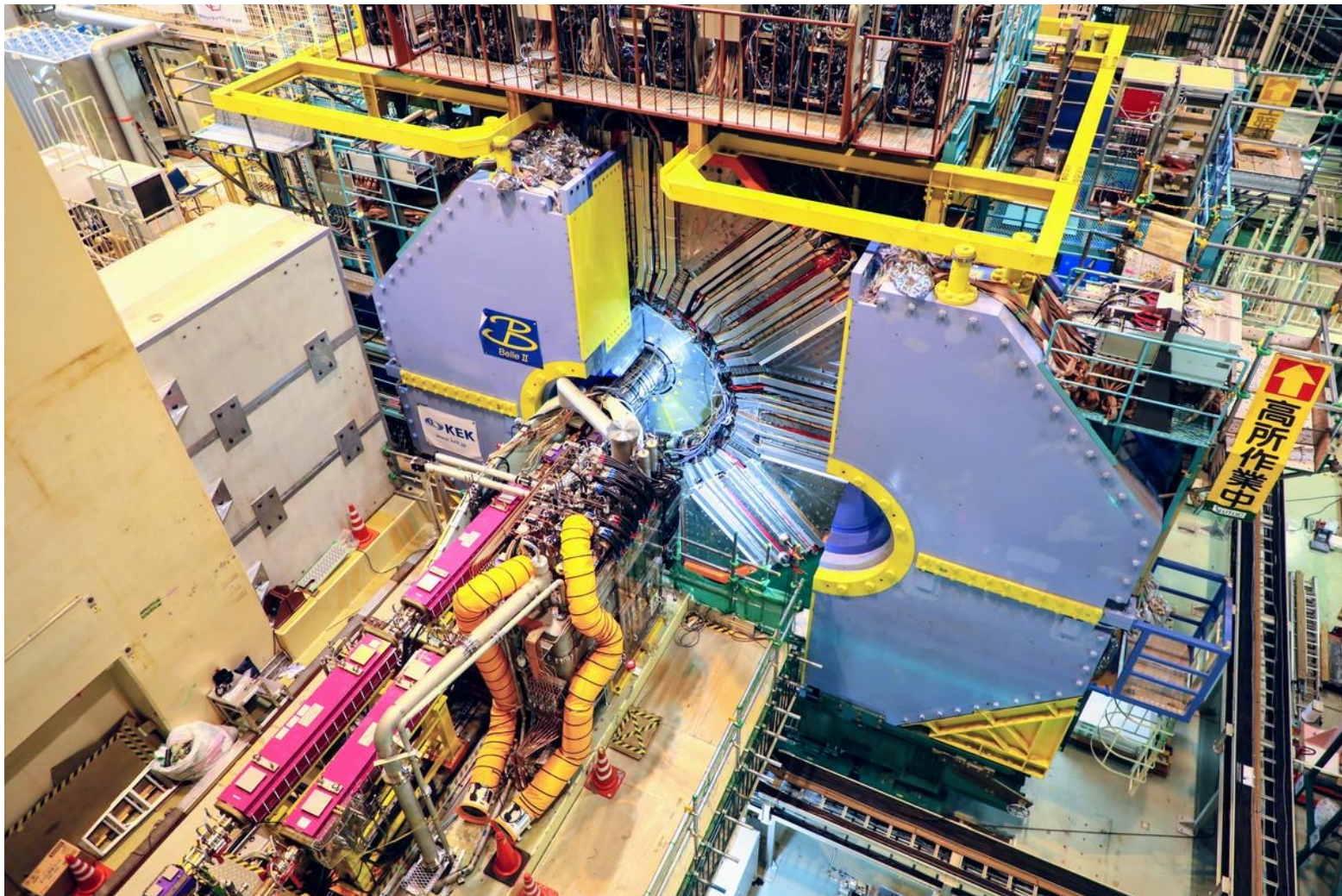
Belle II Experiment

- Upgrade of Belle experiment
- KEK B-factory -> Super KEK B-factory
40 times luminosity (beam current 2 times, beam size 1/20)
- Belle detector -> Belle II detector
More layers of VXD, CDC,
New Tech: TOP counter,
High speed DAQ

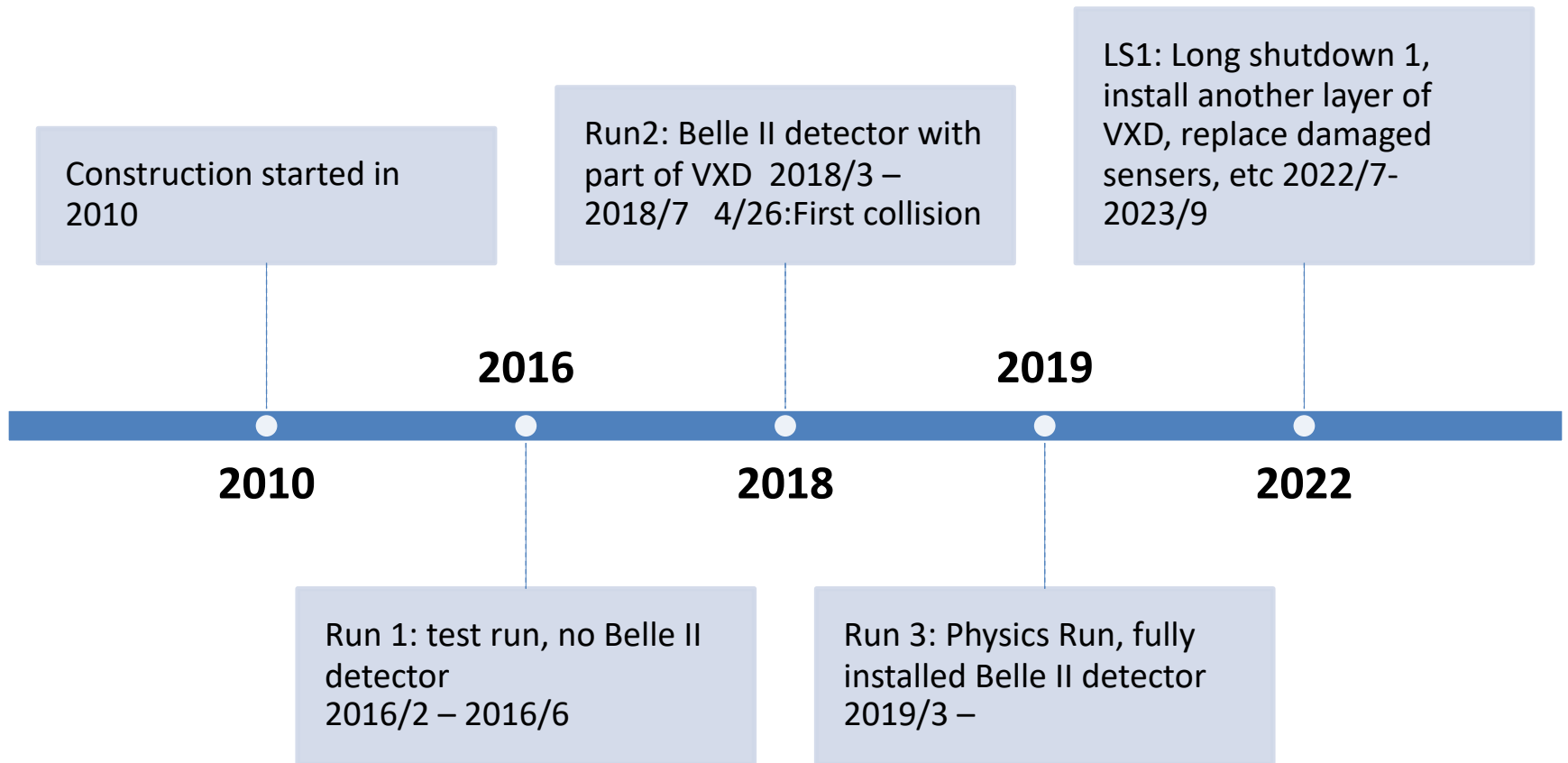
Belle II detector



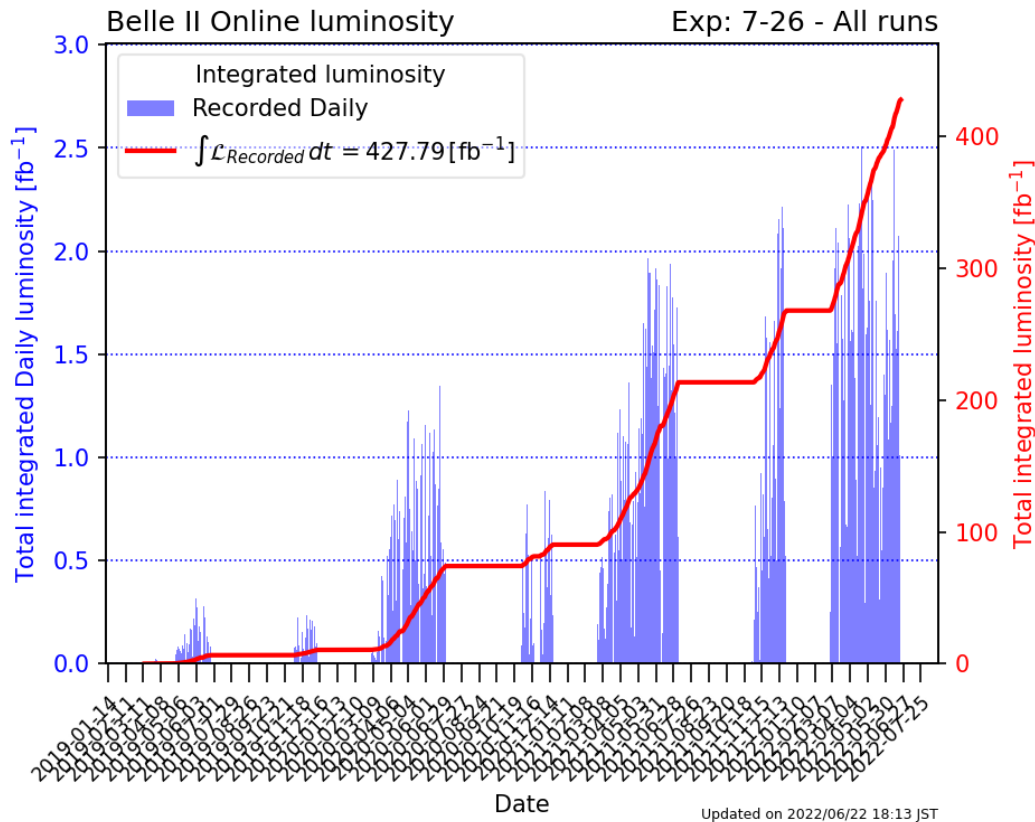
Belle II detector



Time-line of Belle II Experiment

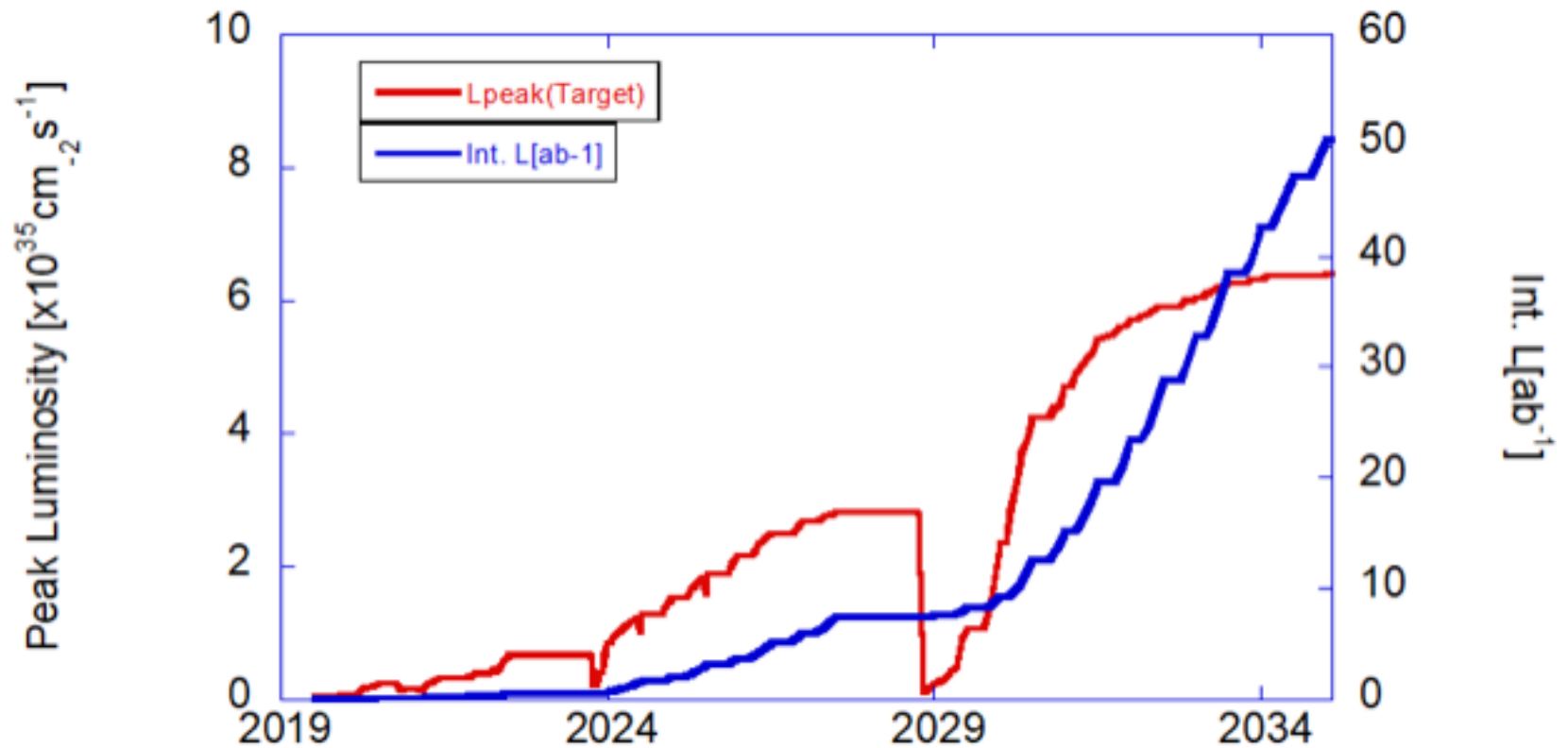


SuperKEKB integrated luminosity



- Total integrated luminosity: **424 fb^{-1}**
- Total integrated luminosity at the $Y(4S)$ resonance: **363 fb^{-1}**
- Total integrated luminosity below $Y(4S)$ resonance: **42 fb^{-1}**
- Total integrated luminosity above $Y(4S)$ resonance: **19 fb^{-1}**

SuperKEKB luminosity projection



Recent results on hadron physics at Belle

$\Omega(2012)$ related

Observation of Excited Ω PRL 121, 052003 (2018)

Evidence for the decay

$\Omega_c \rightarrow \pi^+ \Omega(2012) \rightarrow \pi^+ (\bar{K}E)$ PRD 104, 052005 (2021)

Search for $\Omega(2012) \rightarrow \bar{K}E(1530)$

PRD 100, 032006 (2019)

Observation of $\Omega(2012) \rightarrow \bar{K}E(1530)$

arXiv:2207.03090, Chinese Physics C (accepted)

Observation of Excited Ω

PRL 121, 052003 (2018)

Motivation

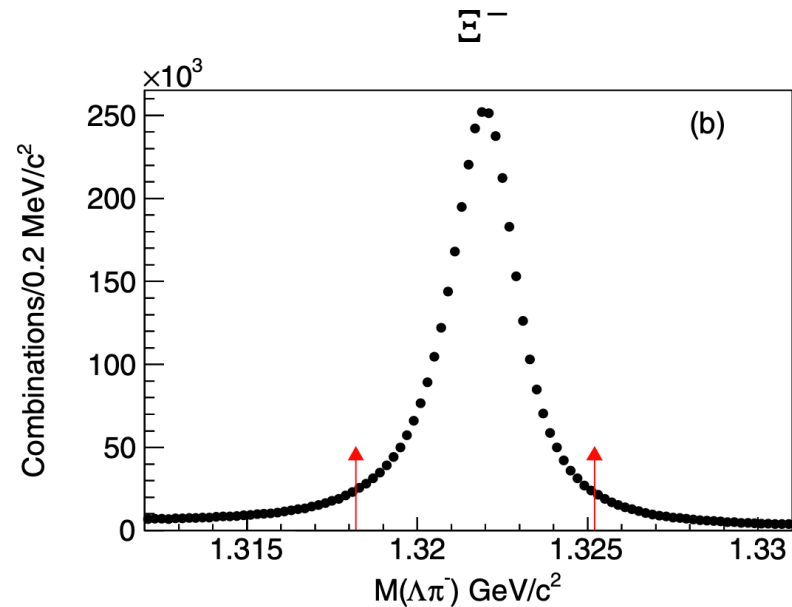
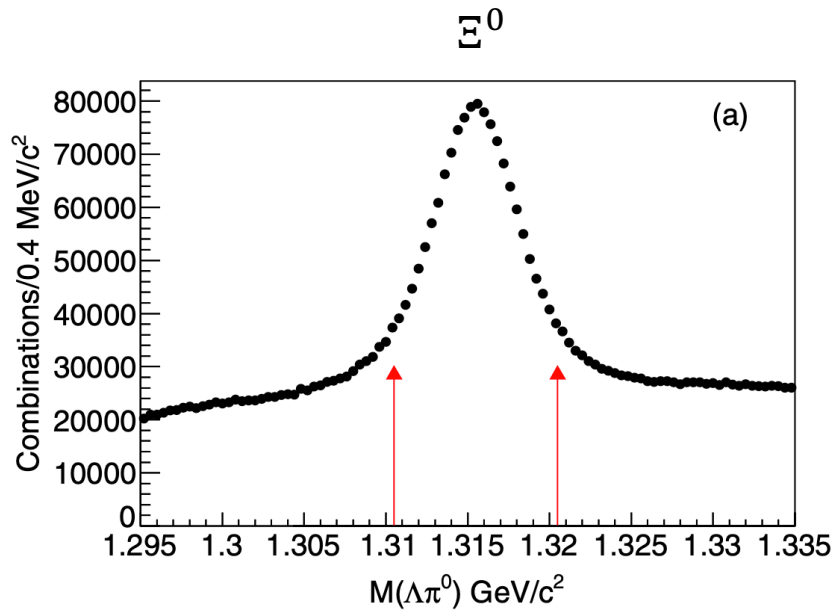
- P-wave excited states of Λ , Σ , and Ξ hyperons have been observed several hundred MeV above the corresponding ground states.
- The excited state of Ω baryons has been found very little.
- The Ω baryon is isospin=0 and therefore $\Omega^{*-} \rightarrow \Omega^- \pi^0$ decay is strongly suppressed.

Data set

- All Belle data 980fb^{-1} was used, but we focused on the following data.
- $\Upsilon(1S)$ data 5.7fb^{-1}
 $\Upsilon(2S)$ data 24.9fb^{-1}
 $\Upsilon(3S)$ data 2.9fb^{-1}
- It has long been known that they contain an enhanced baryon fraction compared with continuum events $e^+e^- \rightarrow q\bar{q}$.

reconstruction

- $\Omega^{*-} \rightarrow \Xi^{-} \bar{K}^0, \Xi^0 K^{-},$
 $\Xi^{-} \rightarrow, \Lambda \pi^{-}, \Xi^0 \rightarrow, \Lambda \pi^0,$
 $\bar{K}^0 \rightarrow \pi^+ \pi^{-}, \Lambda \rightarrow p \pi^{-}$



reconstruction

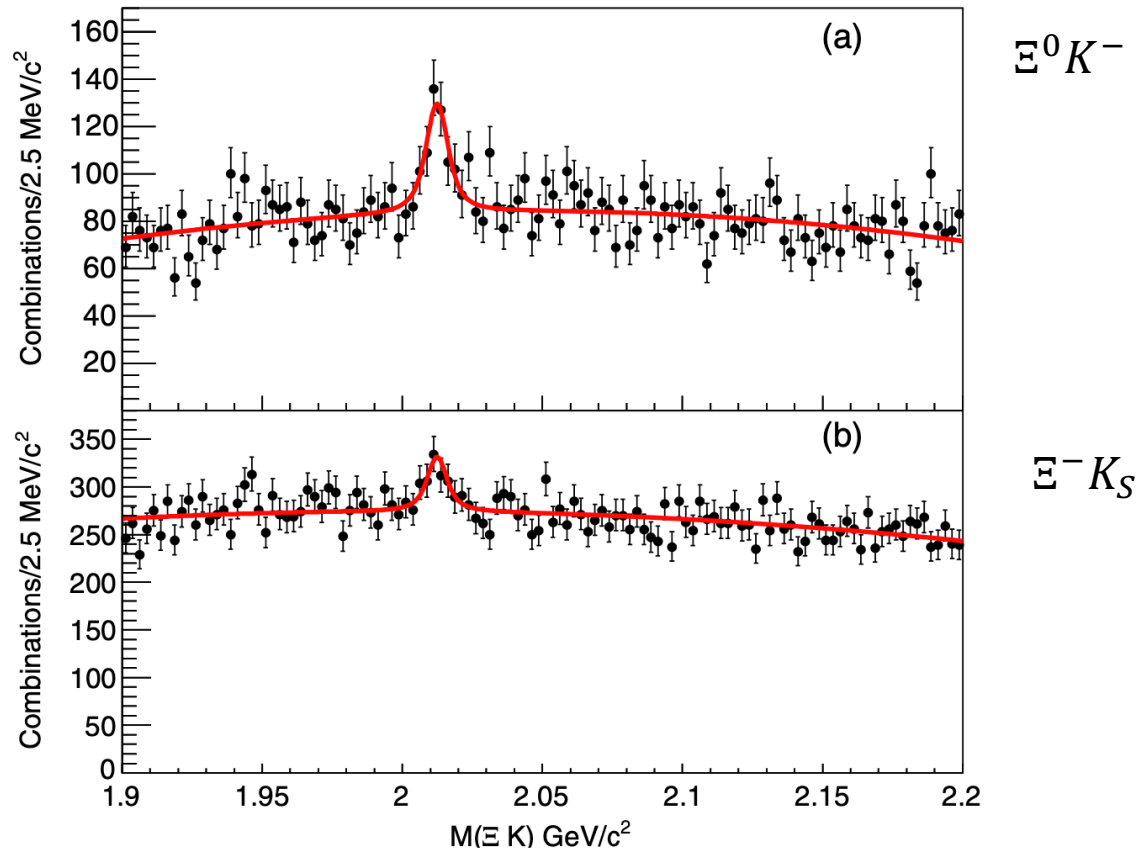


FIG. 2. The (a) $\Xi^0 K^-$ and (b) $\Xi^- K_S^0$ invariant mass distributions in data taken at the $\Upsilon(1S)$, $\Upsilon(2S)$, and $\Upsilon(3S)$ resonance energies. The curves show a simultaneous fit to the two distributions with a common mass and width.

reconstruction

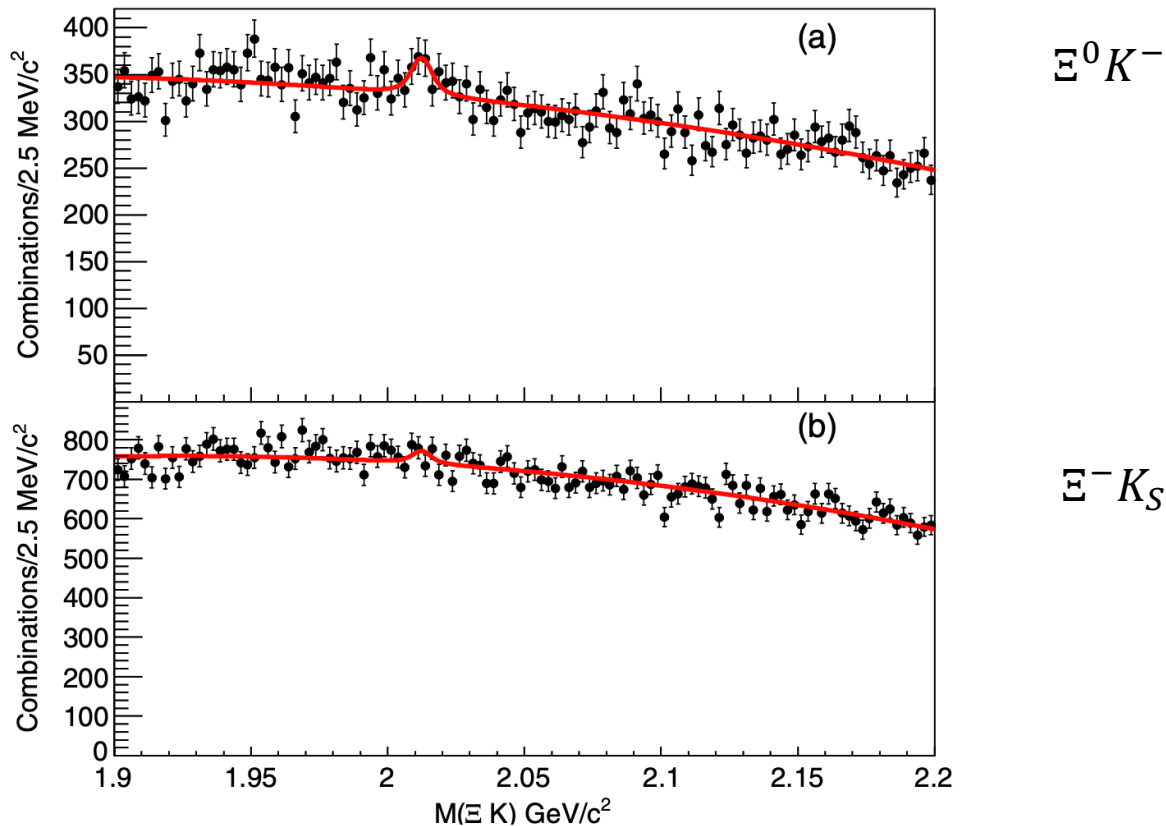


FIG. 3. The (a) $\Xi^0 K^-$, (b) $\Xi^- K_S^0$ invariant mass distributions in data taken at energies other than $\Upsilon(1S)$, $\Upsilon(2S)$, and $\Upsilon(3S)$ resonance energies. The curves show the result of independent fits to the two distributions with masses and widths fixed to those found by the fit shown in Fig. 2.

Results

TABLE I. The results of fits to the data shown in Fig. 2. The uncertainties shown are statistical only.

Data	Mode	Mass (MeV/ c^2)	Yield	Γ (MeV)	χ^2 /d.o.f.	n_σ
$\Upsilon(1S, 2S, 3S)$	$\Xi^0 K^-, \Xi^- K_S^0$ (simultaneous)	2012.4 ± 0.7	$242 \pm 48, 279 \pm 71$	$6.4_{-2.0}^{+2.5}$	227/230	8.3
$\Upsilon(1S, 2S, 3S)$	$\Xi^0 K^-$	2012.6 ± 0.8	239 ± 53	6.1 ± 2.6	115/114	6.9
$\Upsilon(1S, 2S, 3S)$	$\Xi^- K_S^0$	2012.0 ± 1.1	286 ± 87	6.8 ± 3.3	101/114	4.4
Other	$\Xi^0 K^-$	2012.4 (fixed)	209 ± 63	6.4 (fixed)	102/116	3.4
Other	$\Xi^- K_S^0$	2012.4 (fixed)	153 ± 89	6.4 (fixed)	133/116	1.7

Summary

- We found $\Omega(2012)$: a lower excited state of Ω .
- $Y(1S)$, $Y(2S)$, and $Y(3S)$ data are very effective for producing (excited) hyperons.
- Why is the production rate of $\Omega(2012)$ so small in the continuum data?
Is production of ss diquark pair small?

Evidence for the decay

$$\Omega_c \rightarrow \pi^+ \quad \Omega(2012) \rightarrow \pi^+ (\bar{K} \Xi)$$

PRD 104, 052005 (2021)

Motivation

- In order to understand the structure of Ω (2012), studies of other production ways may be useful.
- One candidate is the non-leptonic weak decay of Ω_c .

Data set and analysis modes

- All Belle data 980fb^{-1} was used, but we focused on the following data.
- We performed two analysis modes.

$$\Omega_c^0 \rightarrow \pi^+ \Omega(2012)^- \rightarrow \pi^+ K^- \Xi^0$$

$$\Omega_c^0 \rightarrow \pi^+ \Omega(2012)^- \rightarrow \pi^+ K_S^0 \Xi^-$$

Dalitz plots

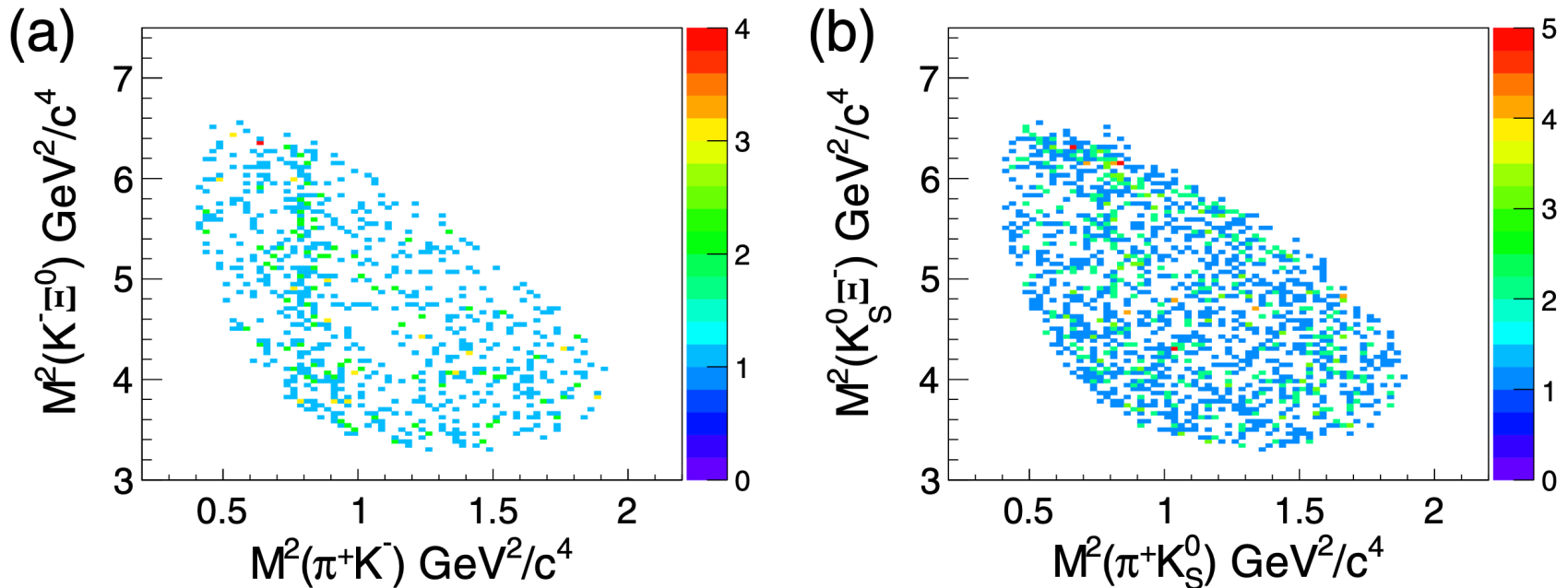


FIG. 1. The Dalitz plots of (a) $M^2(K^- \Xi^0)$ versus $M^2(\pi^+ K^-)$ and (b) $M^2(K_S^0 \Xi^-)$ versus $M^2(\pi^+ K_S^0)$ from selected $\Omega_c^0 \rightarrow \pi^+ K^- \Xi^0$ and $\Omega_c^0 \rightarrow \pi^+ K_S^0 \Xi^-$ candidates.

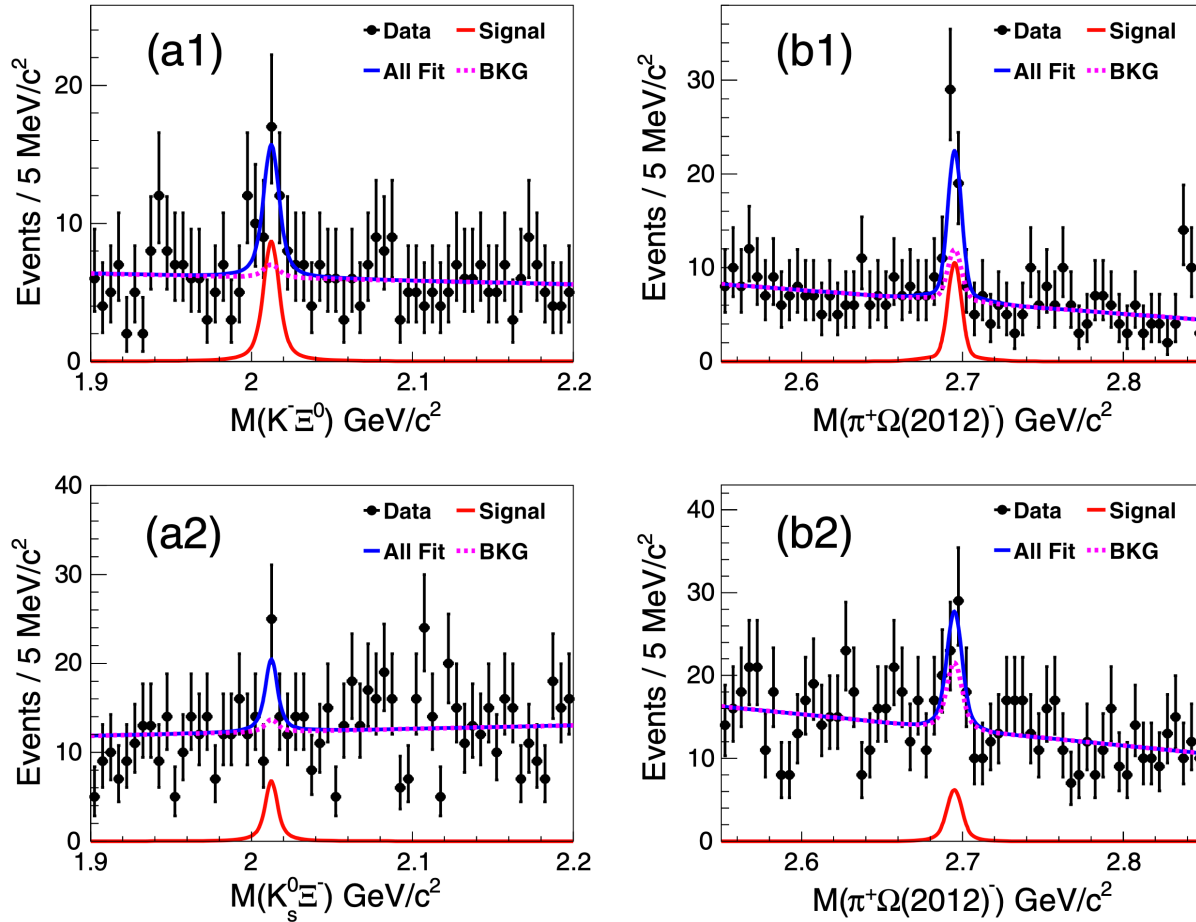


FIG. 2. The 1D projections of the 2D fits of (a) $M(K^- \Xi^0)/M(K_s^0 \Xi^-)$ and (b) $M(\pi^+ \Omega(2012)^-)$ distributions for (1) $\Omega_c^0 \rightarrow \pi^+ \Omega(2012)^- \rightarrow \pi^+ K^- \Xi^0$ and (2) $\Omega_c^0 \rightarrow \pi^+ \Omega(2012)^- \rightarrow \pi^+ K_s^0 \Xi^-$ decays in data. All components are indicated in the legends and described in the text.

Non-resonant 3-body decay

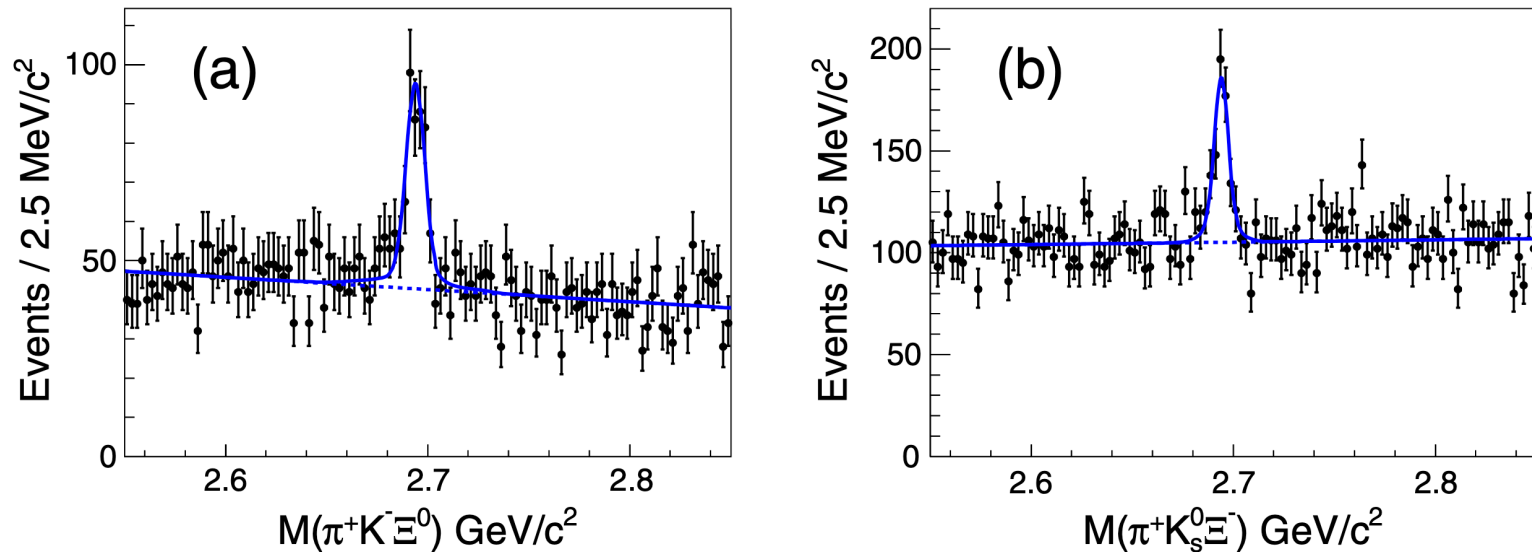


FIG. 3. The (a) $M(\pi^+ K^- \Xi^0)$ and (b) $M(\pi^+ K_s^0 \Xi^-)$ distributions in data. The blue solid curves show the best-fit results, and the blue dashed curves show the fitted backgrounds.

Branching fraction ratios

$$\begin{aligned}
 \mathcal{R}_1 &= \frac{\mathcal{B}(\Omega_c^0 \rightarrow \pi^+ \Omega(2012)^-) \mathcal{B}(\Omega(2012)^- \rightarrow K^- \Xi^0)}{\mathcal{B}(\Omega_c^0 \rightarrow \pi^+ K^- \Xi^0)} \\
 &= \frac{N_{\pi^+ \Omega(2012)^- (\rightarrow K^- \Xi^0)}^{\text{obs}} \times \epsilon_{\pi^+ K^- \Xi^0}}{N_{\pi^+ K^- \Xi^0}^{\text{obs}} \times \epsilon_{\pi^+ \Omega(2012)^- (\rightarrow K^- \Xi^0)}} \\
 &= (9.6 \pm 3.2(\text{stat.}) \pm 1.8(\text{syst.}))\%,
 \end{aligned}$$

$$\begin{aligned}
 \mathcal{R}_2 &= \frac{\mathcal{B}(\Omega_c^0 \rightarrow \pi^+ \Omega(2012)^-) \mathcal{B}(\Omega(2012)^- \rightarrow \bar{K}^0 \Xi^-)}{\mathcal{B}(\Omega_c^0 \rightarrow \pi^+ \bar{K}^0 \Xi^-)} \\
 &= \frac{N_{\pi^+ \Omega(2012)^- (\rightarrow K_S^0 \Xi^-)}^{\text{obs}} \times \epsilon_{\pi^+ K_S^0 \Xi^-}}{N_{\pi^+ K_S^0 \Xi^-}^{\text{obs}} \times \epsilon_{\pi^+ \Omega(2012)^- (\rightarrow K_S^0 \Xi^-)}} \\
 &= (5.5 \pm 2.8(\text{stat.}) \pm 0.7(\text{syst.}))\%.
 \end{aligned}$$

Signal yields

TABLE I. Summary of the fitted signal yields (N^{obs}) and reconstruction efficiencies (ϵ). All the uncertainties here are statistical only.

Mode	N^{obs}	$\epsilon(\%)$
$\Omega_c^0 \rightarrow \pi^+ \Omega(2012)^- \rightarrow \pi^+ K^- \Xi^0$	28.3 ± 8.9	3.59
$\Omega_c^0 \rightarrow \pi^+ \Omega(2012)^- \rightarrow \pi^+ K_S^0 \Xi^-$	17.9 ± 8.9	7.68
$\Omega_c^0 \rightarrow \pi^+ K^- \Xi^0$	279 ± 27	3.41
$\Omega_c^0 \rightarrow \pi^+ K_S^0 \Xi^-$	317 ± 32	7.41

Two modes combined results

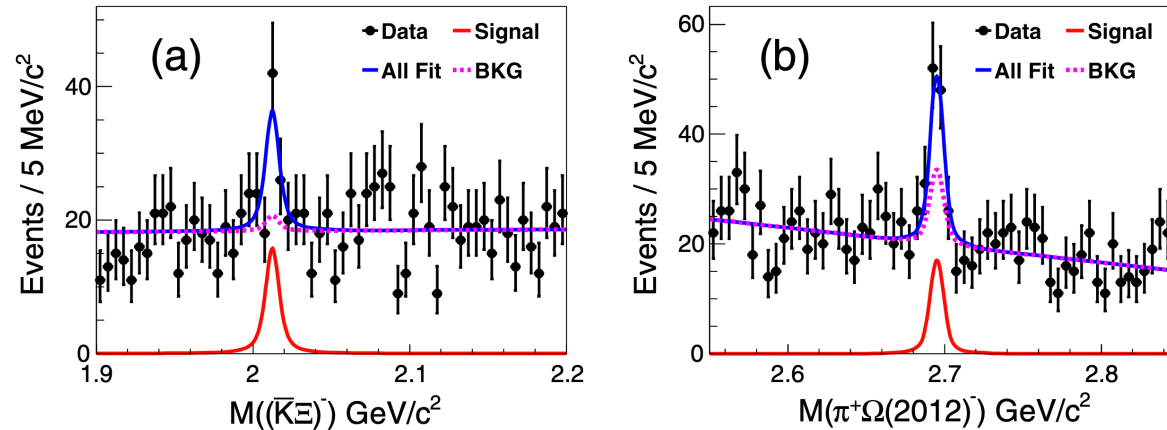


FIG. 4. The 1D projections of the 2D simultaneous fit of (a) $M((\bar{K}\Xi)^-)$ and (b) $M(\pi^+\Omega(2012)^-)$ distributions in data. All components are indicated in the legends and described in the text.

Total signal yield: 46.6 ± 12.3

Statistical significance: 4.6σ

Signal significance with systematic uncertainties included: 4.2σ

Observation for $\Omega(2012) \rightarrow \bar{K}\Xi(1530)$

PRD 100, 032006 (2019)

Observation of $\Omega(2012) \rightarrow \bar{K}\Xi(1530)$

arXiv:2207.03090, Chinese Physics C (accepted)

Motivation

- Structure of $\Omega(2012)^-$
- Conventional:
sss P-wave excited state $J^P = 3/2^-$
 $\Omega(2012)^- \rightarrow K \Xi$ is D-wave decay, which is consistent with the observed small width.
- Exotic:
K $\Xi(1530)$ hadronic molecule
Threshold: $1531.80 + 493.68 = 2025.48$ MeV
Expected large $K \pi \Xi$ decay width.

Data set and 2019 analysis modes

- $\Upsilon(1S)$ data 5.7 fb^{-1} 102 million $\Upsilon(1S)$
- $\Upsilon(2S)$ data 24.9 fb^{-1} 158 million $\Upsilon(2S)$
- $\Upsilon(3S)$ data 2.9 fb^{-1} 12 million $\Upsilon(3S)$

- Analysis mode

$$\Omega(2012)^- \rightarrow \Xi(1530)^0 (\rightarrow \Xi^- \pi^+) K^-$$

$$\Omega(2012)^- \rightarrow \Xi(1530)^- (\rightarrow \Xi^- \pi^0) K_S^0$$

$$\Omega(2012)^- \rightarrow \Xi(1530)^- (\rightarrow \Xi^0 \pi^-) K_S^0$$

$$\Omega(2012)^- \rightarrow \Xi(1530)^0 (\rightarrow \Xi^0 \pi^0) K^-$$

Cut

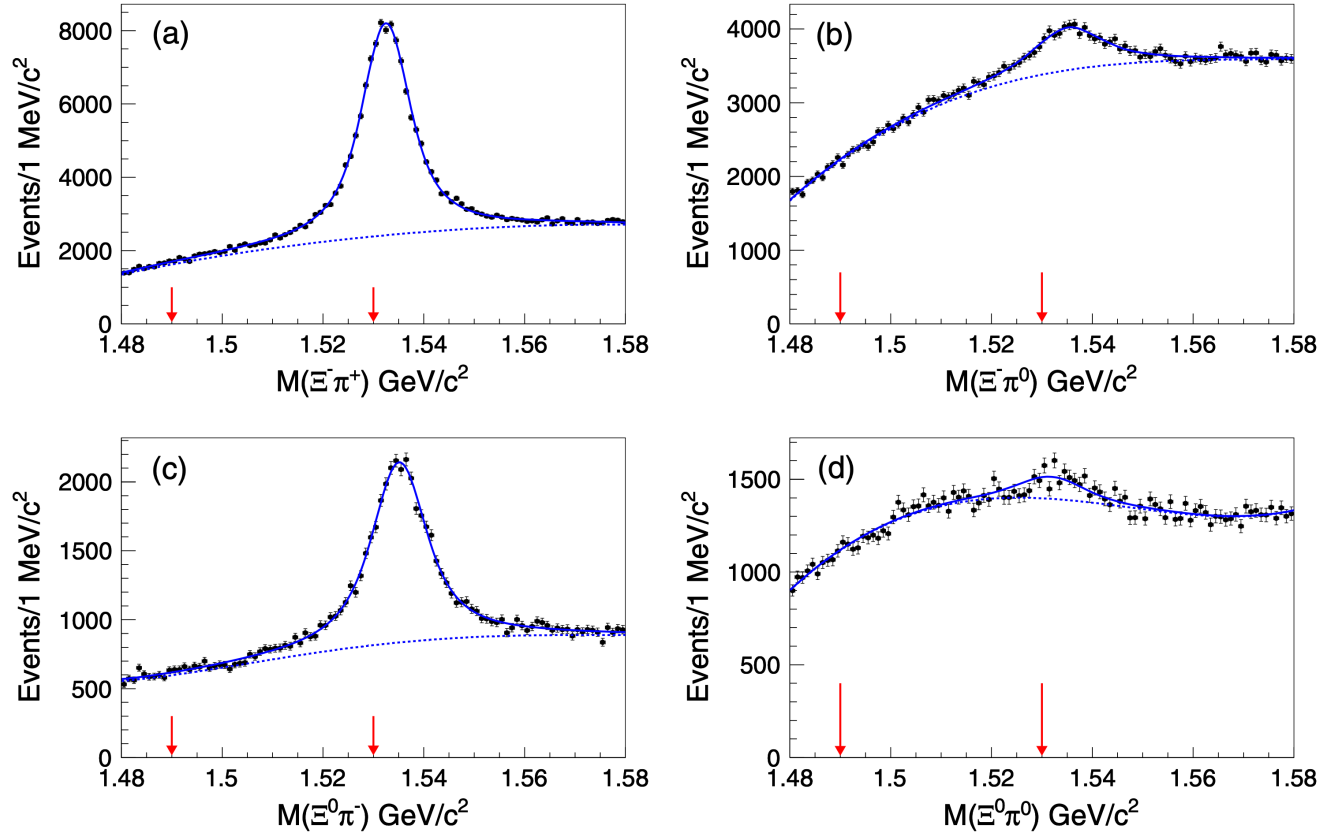


FIG. 3. Invariant mass distributions for (a) $\Xi(1530)^0 \rightarrow \Xi^- \pi^+$, (b) $\Xi(1530)^- \rightarrow \Xi^- \pi^0$, (c) $\Xi(1530)^- \rightarrow \Xi^0 \pi^-$, and (d) $\Xi(1530)^0 \rightarrow \Xi^0 \pi^0$ candidates from the $\Upsilon(1S, 2S, 3S)$ data samples. Solid curves are the best fits, and dashed lines represent backgrounds. Red arrows indicate the $\Xi(1530)$ signal region for the $\Omega(2012)$ search, which is offset from the peak owing to the very limited allowed phase space.

Results

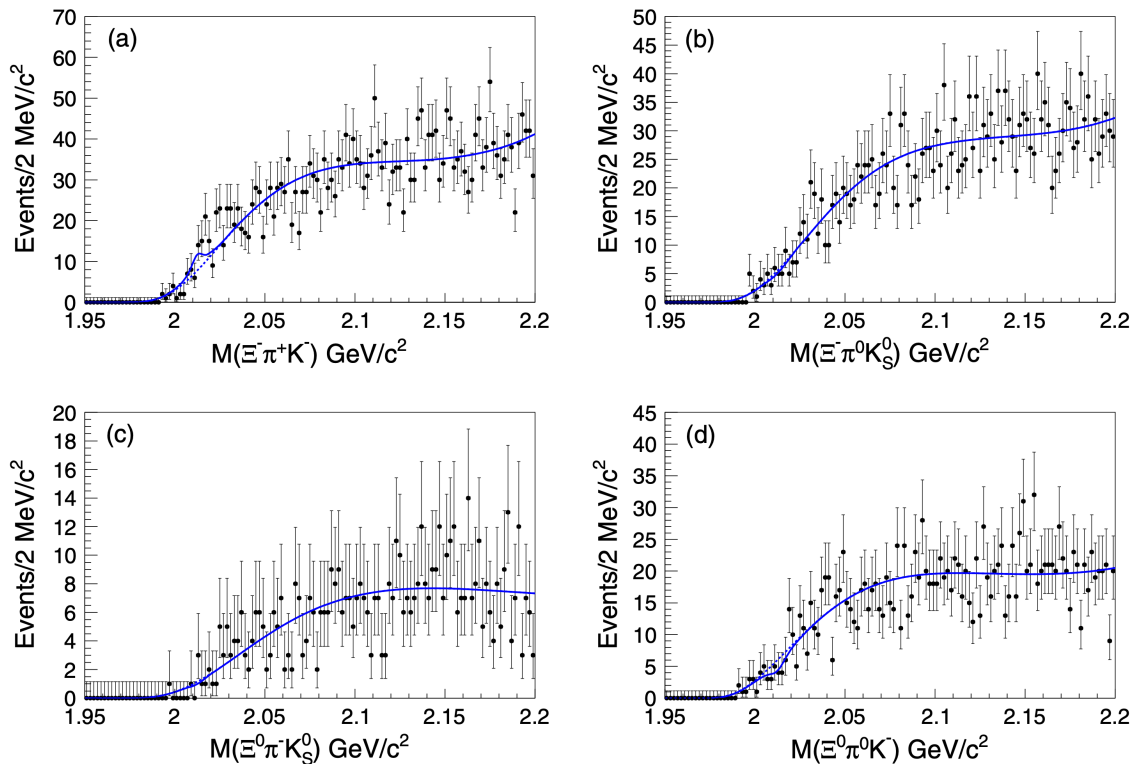


FIG. 4. The distributions of the invariant mass for (a) $\Xi(1530)^0 \rightarrow \Xi^- \pi^+ K^-$, (b) $\Xi(1530)^- \rightarrow \Xi^- \pi^0 K_S^0$, (c) $\Xi(1530)^- \rightarrow \Xi^0 \pi^- K_S^0$, and (d) $\Xi(1530)^0 \rightarrow \Xi^0 \pi^0 K^-$ from the $\Upsilon(1S, 2S, 3S)$ data samples. The solid curves are the best fits, and the dashed lines represent the backgrounds.

No significant signals are observed.

Data set and 2022 analysis modes

- $\Upsilon(1S)$ data 5.7 fb^{-1} 102 million $\Upsilon(1S)$
 $\Upsilon(2S)$ data 24.9 fb^{-1} 158 million $\Upsilon(2S)$
 $\Upsilon(3S)$ data 2.9 fb^{-1} 12 million $\Upsilon(3S)$
- Analysis mode

$$\Omega(2012)^- \rightarrow \Xi(1530)^0 (\rightarrow \Xi^- \pi^+) K^-$$

New Cut

- We require $M(\Xi^- \pi^+) < 1.517 \text{ GeV}$ to improve the signal-to-background ratio.

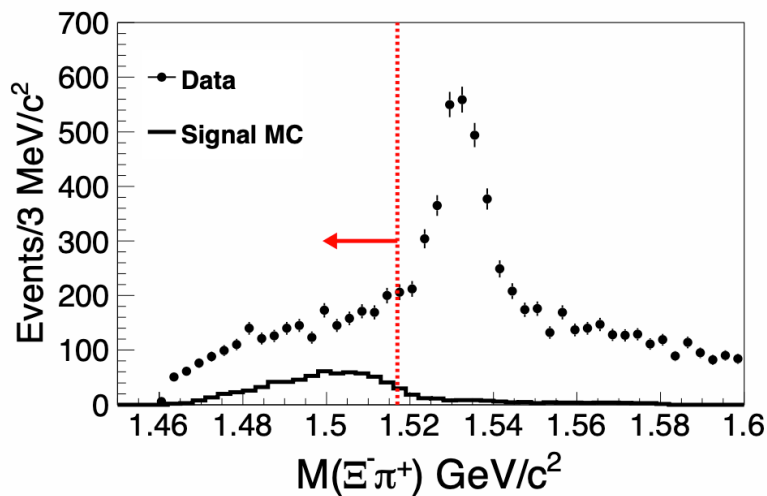


FIG. 1: The mass distributions of $\Xi^- \pi^+$ in $\Omega(2012)^- \rightarrow \Xi(1530)^0 K^- \rightarrow \Xi^- \pi^+ K^-$ from the signal MC sample and $\Upsilon(1S)$, $\Upsilon(2S)$, and $\Upsilon(3S)$ data. The number of signal-MC events is scaled to three times the yield of $\Omega(2012)^- \rightarrow \Xi^- \pi^+ K^-$ in data to make it more visible. The red arrow shows $M(\Xi^- \pi^+) < 1.517 \text{ GeV}$.

Mass spectra

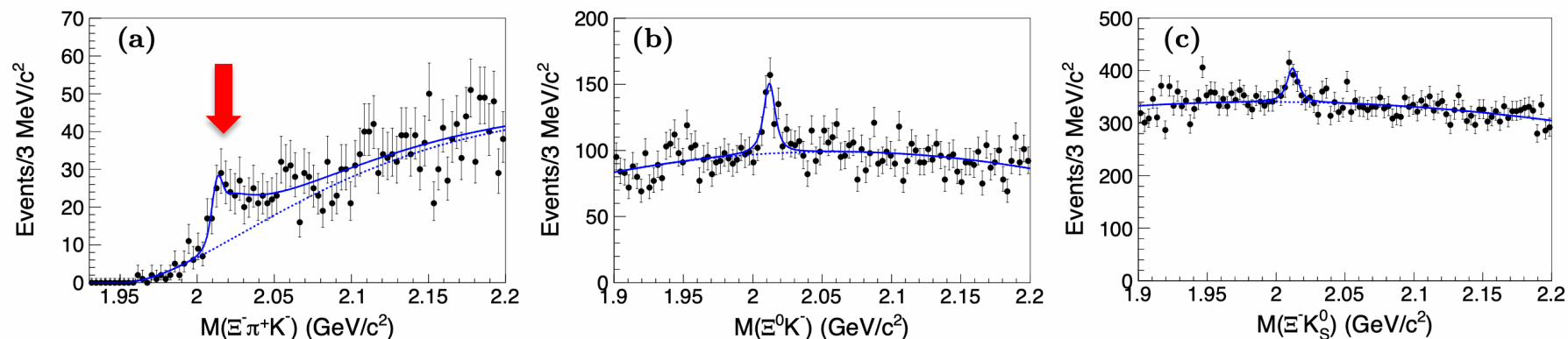


FIG. 2: The mass spectra of (a) $\Xi^- \pi^+ K^-$, (b) $\Xi^0 K^-$, and (c) $\Xi^- K_S^0$ in data. The solid curves are the best fits, and the dashed curves are backgrounds.

$\Omega(2012)^- \rightarrow \Xi^- \pi^+ K^-$ yield: 263 ± 53

Statistical significance: 5.6σ

Signal significance with systematic uncertainties included: 5.2σ


Branching fraction ratios

$$\mathcal{R}_{\Xi^- \bar{K}^0}^{\Xi^- \pi^+ K^-} = 0.69 \pm 0.21 \pm 0.03,$$

$$\mathcal{R}_{\Xi^0 K^-}^{\Xi^- \pi^+ K^-} = 0.61 \pm 0.16 \pm 0.04,$$

$$\mathcal{R}_X^{\Xi^- \pi^+ K^-} = \frac{\mathcal{B}(\Omega(2012)^- \rightarrow \Xi(1530)^0 K^- \rightarrow \Xi^- \pi^+ K^-)}{\mathcal{B}(\Omega(2012)^- \rightarrow X)}$$

Assumption



We assume all $\Xi^- \pi^+$ events are from $\Xi(1530)^0$.

If this assumption is good, then present result seems to be consistent with hadronic molecule picture.

The conventional sss picture and hybrid picture are not excluded.

Spin-parity of $\Xi_c(2970)$

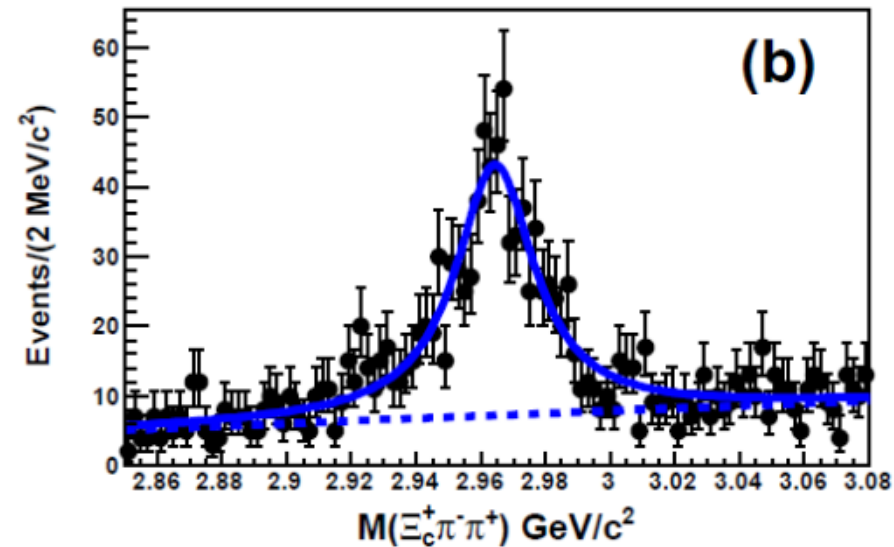
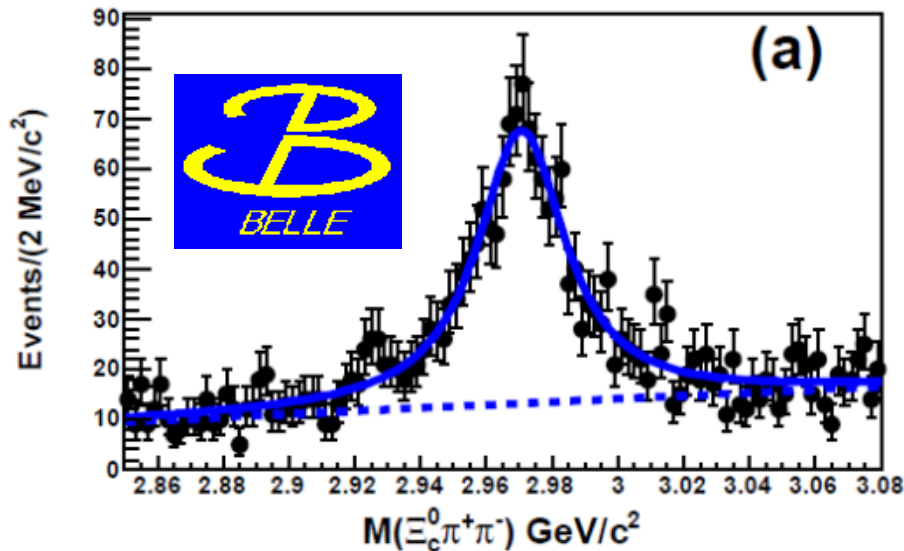
PRD 103, L111101 (2021)

Taken from Tanida-san's slides presented at NSTAR2022

$\Xi_c(2970)$

- Relatively low excitation energy
 - Good statistics & S/N ratio

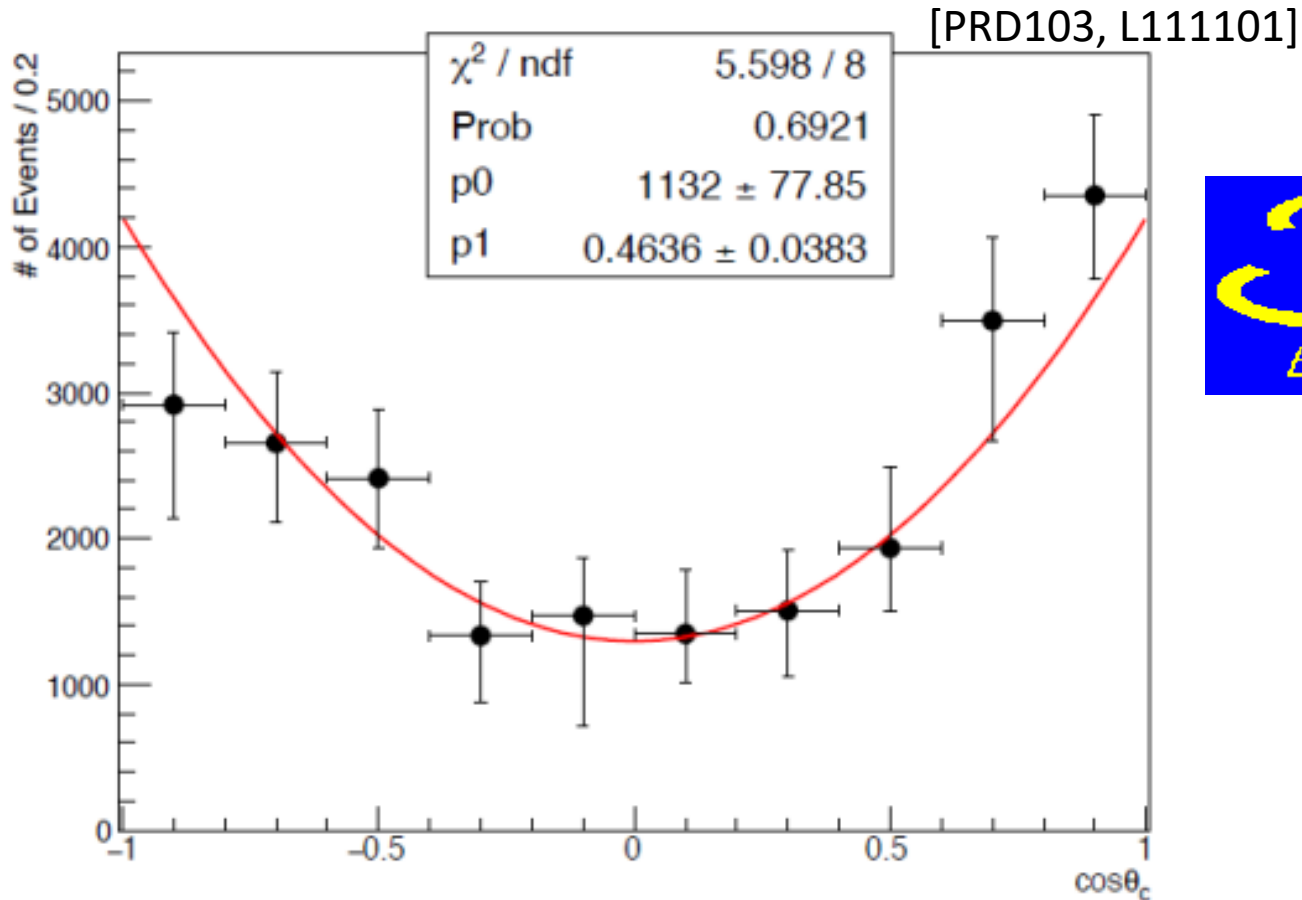
Belle, PRD94, 052011 (2016)



- Wide variety of theoretical predictions
- Important decay mode: $\Xi_c(2970) \rightarrow \Xi_c^*(2645)\pi$

SPIN: Angular correlation of

$$\Xi_c(2970) \rightarrow \Xi_c^*(2645)\pi_1 \rightarrow \Xi_c\pi_1\pi_2$$



- Consistent with $1+3\cos^2\theta \rightarrow J = 1/2$

[see also: Arifi, Hosaka, Nagahiro, and Tanida, PRD101, 111502(R)(2020)]

PARITY: Decay to $\Xi_c^* \left(3/2^+\right)$ and $\Xi_c' \left(1/2^+\right)$

- $R = \frac{\Gamma(\Xi_c(2970) \rightarrow \Xi_c^* \pi)}{\Gamma(\Xi_c(2970) \rightarrow \Xi_c' \pi)}$ is expected to be small for

negative parity:

- $\Xi_c(2970) \rightarrow \Xi_c' \pi$ is in S-wave, while
 $\Xi_c(2970) \rightarrow \Xi_c^* \pi$ is in D-wave.

- For positive parity, calculable based on HQS

Parity	+	+
Diquark spin s_ℓ	0	1
R	1.06	0.26

- We got $R = 1.67 \pm 0.29(\text{stat.})_{-0.09}^{+0.15}(\text{syst.}) \pm 0.25(\text{IS})$

Discussion

- We got $J^P=1/2^+$. What can we say from this?
- This is **the same as infamous Roper resonance**, $N(1440)$, the first excited state of nucleon.
 - Excitation energy (~ 500 MeV) is also the same.
- Difficult to explain Roper in quark model
 - Single quark excitation: 1st excited state should be a negative parity state (ex. $N(1530)$).
 - Surprisingly, difficult even in Lattice QCD.
 - **The present measurement may give a hint.**

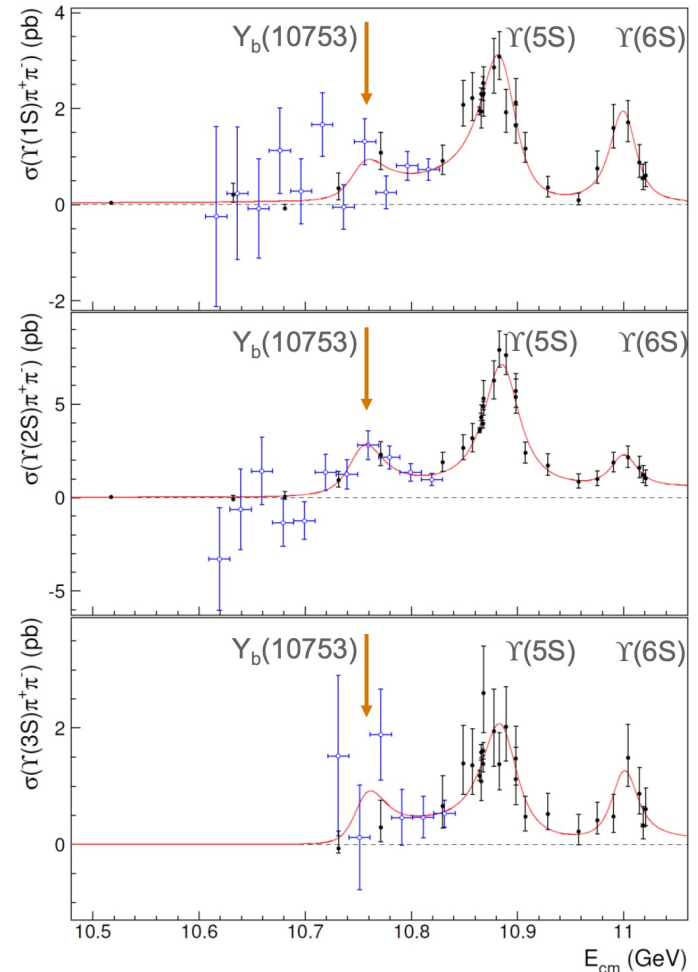
Recent results on hadron physics at Belle II

Observation of $e^+e^- \rightarrow \omega\chi_{bJ}(1P)$
and
search for $X_b \rightarrow \omega\Upsilon(1S)$
at \sqrt{s} near 10.75 GeV

arXiv:2208.13189

Motivation

- What is $Y_b(10753)$ ($Y(10753)$)?
- $Y_b(10753)$ is sitting between $Y(4S)$ and $Y(5S)$.
- GI estimation of $Y(3D)$ is 10.70 GeV
- PRD93, 074027 (2016) estimation of $Y(3D)$ is 10.653 GeV



JHEP 10 (2019) 220

Motivation

- Conventional bottomonium with large S-D mixing is expected to give comparable order of branching fractions for $\Upsilon(10753) \rightarrow \omega \chi_{bJ}(1P)$ and $\Upsilon(10753) \rightarrow \pi^+ \pi^- \Upsilon(nS)$.
- (Mechanism of large S-D mixing is not discussed.)

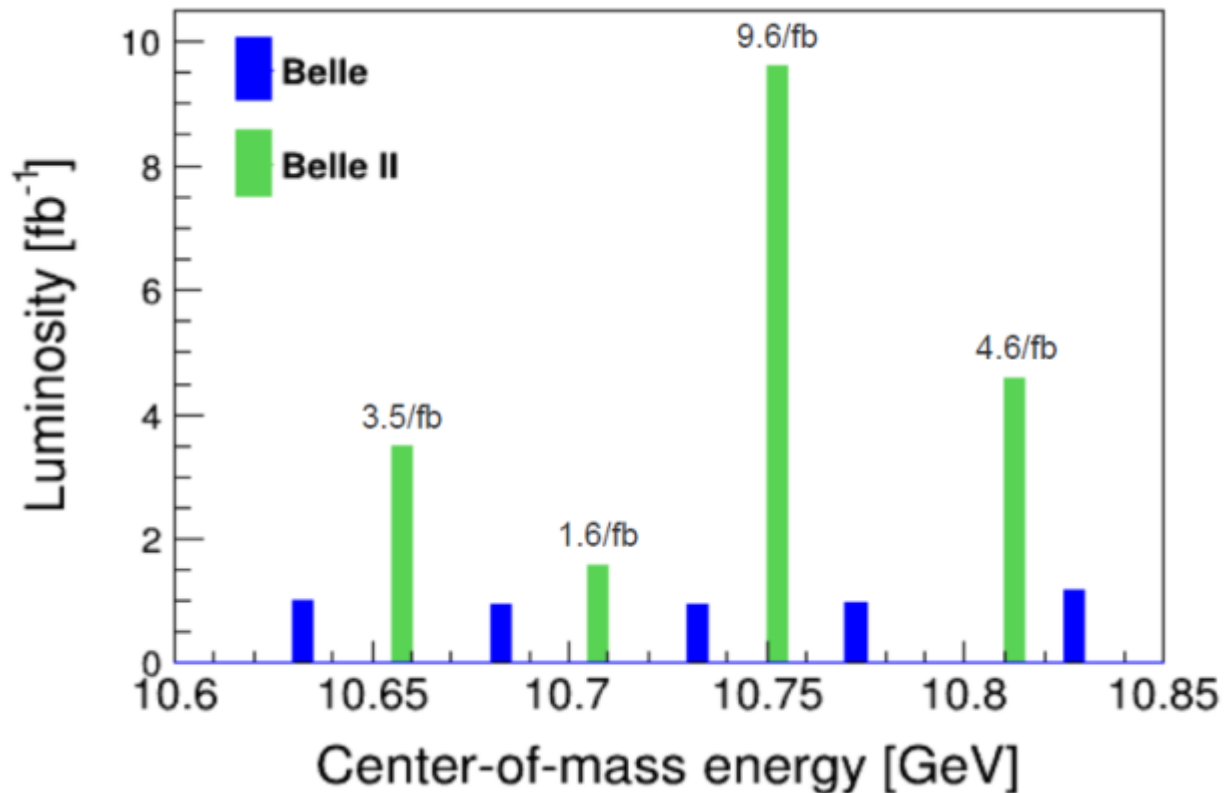
Motivation

- Since χ_{bJ} is reconstructed by $\gamma Y(1S)$, we can search $X_b \rightarrow \omega Y(1S)$ in the same process:

$$Y(10753) \rightarrow \omega \chi_{bJ}(1P) \rightarrow \omega \gamma Y(1S)$$

Energy Scan

- We took data near 10.75 GeV in Nov. 2021.



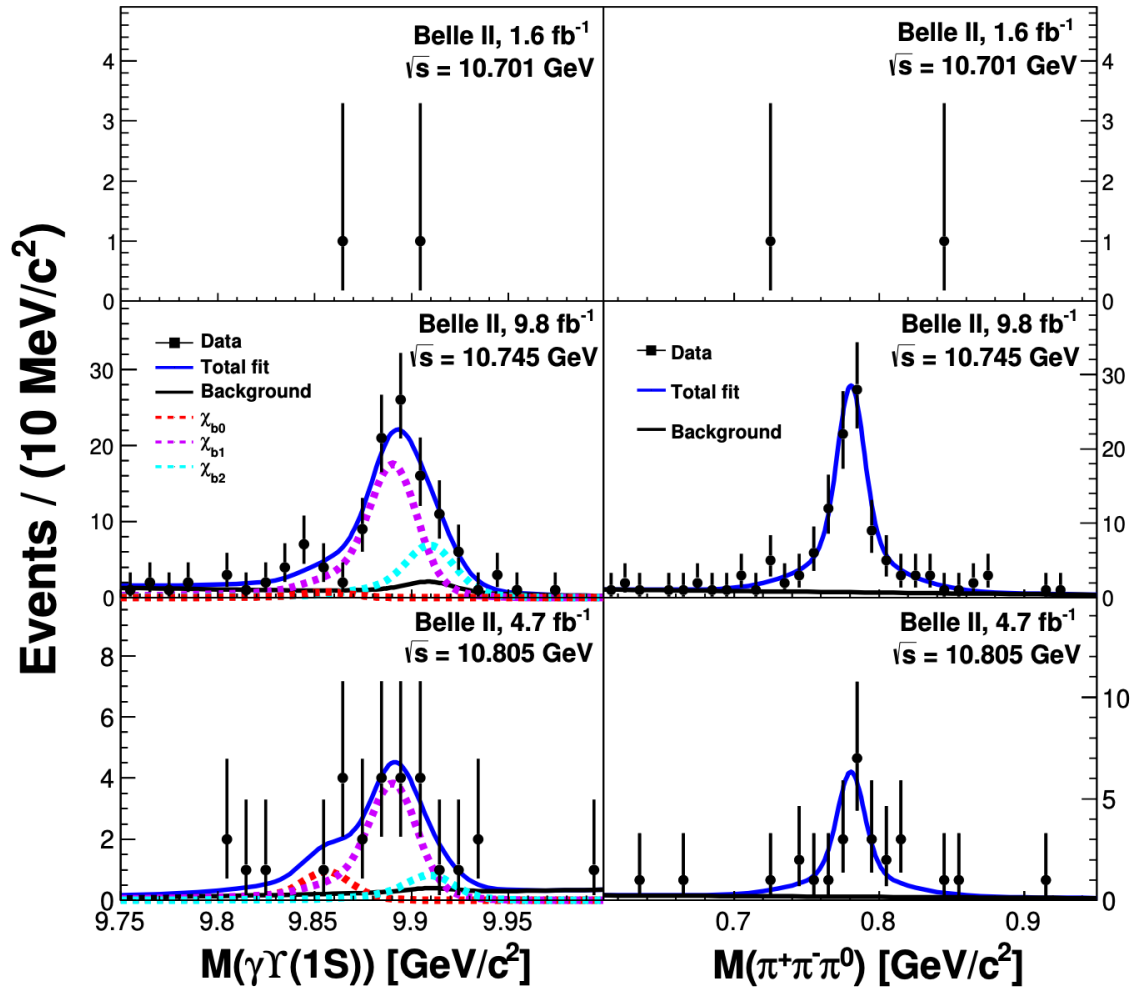


FIG. 1: Distributions of (left) $\gamma\Upsilon(1S)$ and (right) $\pi^+\pi^-\pi^0$ masses in data at $\sqrt{s} = 10.701, 10.745,$ and 10.805 GeV with fit results overlaid.

TABLE I: Measurements of $e^+e^- \rightarrow \omega\chi_{bJ}$ at $\sqrt{s} = 10.701, 10.745,$ and 10.805 GeV. Σ is the signal significance; Syst is the systematic uncertainty. The first and second uncertainties (if available) indicate statistical and systematic contributions, respectively. The common systematic uncertainties for all energy points are 15.8%, 9.4%, and 9.3% for $\omega\chi_{b0}, \omega\chi_{b1},$ and $\omega\chi_{b2},$ respectively.

Channel	\sqrt{s} (GeV)	N^{sig}	N^{UL}	$\Sigma(\sigma)$	ϵ	$ 1 - \Pi ^2$	$1 + \delta_{\text{ISR}}$	Syst (%)	σ_B (pb)	σ_B^{UL} (pb)
$e^+e^- \rightarrow \omega\chi_{b0}$	10.701	$0.0^{+1.1}_{-0.0}$	3.0	-	0.182	0.931	0.67	16.6	$0.0^{+6.1}_{-0.0}$	16.6
$e^+e^- \rightarrow \omega\chi_{b1}$		$0.0^{+2.1}_{-0.0}$	3.9	-	0.184	0.931	0.64	10.6	$0.0^{+0.7}_{-0.0}$	1.2
$e^+e^- \rightarrow \omega\chi_{b2}$		$0.1^{+2.2}_{-0.1}$	4.0	-	0.182	0.931	0.62	10.6	$0.1^{+1.4}_{-0.1}$	2.5
$e^+e^- \rightarrow \omega\chi_{b0}$	10.745	$3.0^{+5.5}_{-4.7}$	12.0	0.5	0.183	0.931	0.65	25.9	$2.8^{+5.1}_{-4.4} \pm 0.7$	11.3
$e^+e^- \rightarrow \omega\chi_{b1}$		$68.9^{+13.7}_{-13.5}$	-	5.9	0.183	0.931	0.65	12.7	$3.6^{+0.7}_{-0.7} \pm 0.5$	-
$e^+e^- \rightarrow \omega\chi_{b2}$		$27.6^{+11.6}_{-10.0}$	-	3.1	0.184	0.931	0.65	14.5	$2.8^{+1.2}_{-1.0} \pm 0.4$	-
$e^+e^- \rightarrow \omega\chi_{b0}$	10.805	$3.6^{+3.8}_{-3.1}$	9.9	1.2	0.182	0.932	1.12	24.9	$4.1^{+4.3}_{-3.5} \pm 1.0$	11.4
$e^+e^- \rightarrow \omega\chi_{b1}$		$15.0^{+6.8}_{-6.2}$	26.2	2.7	0.182	0.932	1.12	20.2	$0.9^{+0.4}_{-0.4} \pm 0.2$	1.7
$e^+e^- \rightarrow \omega\chi_{b2}$		$3.3^{+5.3}_{-3.8}$	12.8	0.8	0.183	0.932	1.11	29.1	$0.4^{+0.7}_{-0.5} \pm 0.1$	1.6

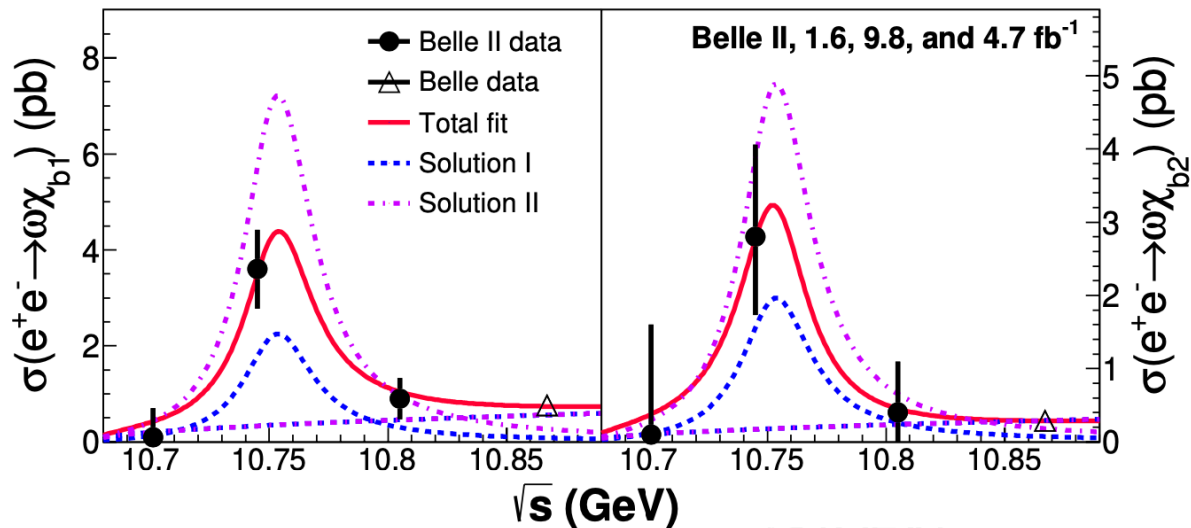


FIG. 2: Energy dependence of the Born cross sections for (left) $e^+e^- \rightarrow \omega\chi_{b1}$ and (right) $e^+e^- \rightarrow \omega\chi_{b2}$. Circles show the measurements reported here, triangles are the results of the Belle experiment [41]. Error bars represent combined statistical and systematic uncertainties. Curves show the fit results and various components of the fit function.

Cross section at $\Upsilon(10860)$ energy is very small compared to one at $\Upsilon(10753)$.
 The structure of $\Upsilon(10860)$ must be quite different from that of $\Upsilon(10753)$.

- $\frac{\sigma_B(e^+e^- \rightarrow \omega \chi_{b1})}{\sigma_B(e^+e^- \rightarrow \omega \chi_{b2})} = 1.3 \pm 0.6$ at $\sqrt{s} = 10.745$ GeV

Theoretical prediction is 15 for a pure D-wave bottomonium. Therefore, $\Upsilon(10753)$ does not seem to be a pure D-wave bottomonium.

Search for $X_b \rightarrow \omega\Upsilon(1S)$

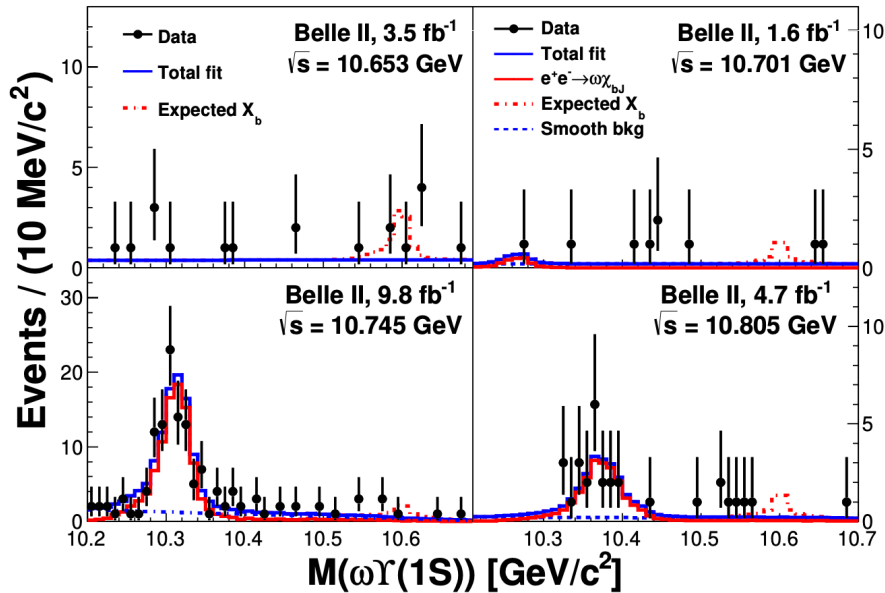


FIG. 3: Distributions of $\omega\Upsilon(1S)$ mass from data at $\sqrt{s} = 10.653, 10.701, 10.745,$ and 10.805 GeV. The red dash-dotted histograms are from simulated events $e^+e^- \rightarrow \gamma X_b (\rightarrow \omega\Upsilon(1S))$ with the X_b mass fixed at 10.6 GeV/c^2 and yields fixed at the upper limit values.

No evidence of a X_b signal is obtained for X_b masses between 10.45 and 10.65 GeV .

We need more data for X_b search.

Belle Summary

- Although the data taking was finished on June 30, 2010, there may be rich physics to be analyzed in Belle data.
- Other recent hadron physics results are shown in the following slides.

Other recent hadrons physics results from Belle

- $e^+e^- \rightarrow \Sigma^0 \Sigma^0$ and $\Sigma^+ \Sigma^-$ by ISR, [arXiv:2210.16761]
- $\Lambda\pi^+$ and $\Lambda\pi^+$ near KN (I=1) threshold, [arXiv:2211.11151]
- $e^+e^- \rightarrow \eta\phi$ by ISR, [arXiv:2209.00810, PRD accepted]
- Threshold cusp at $\Lambda\eta$ in pK^- spectrum, [arXiv:2209.00050]
- a new excited charmed baryon decaying to $\Sigma_c(2455)^{0,++}\pi^\pm$, [arXiv:2206.08822]
- Search for $X(3872) \rightarrow \pi^+\pi^-\pi^0$, [arXiv:2206.08592, PRD accepted]
- $\gamma\gamma \rightarrow \chi_{c1}(1P) \rightarrow J/\psi\gamma$, [arXiv:2208.04477, JHEP accepted]
- Search for $X_{cc\bar{s}\bar{s}}$ in $D_S^{(*)+} D_S^{(*)-}$, [PRD 105, 032002 (2022)]
- Two-particle correlations of hadrons, [PRL 128, 142005 (2022)]

Belle II Summary

- Physics analysis just started!
- We continue data taking and tuning of SuperKEKB to improve luminosity in the covid-19 era.
- We develop new analysis tools including the application of AI technology.

Using large data $\sim 10/\text{ab}$

- Study of double charm hadrons
- Study of radiative decays of XY 's
- Full amplitude analysis of heavy hadron decays and determinations of spin and parity of heavy hadrons
- We welcome your suggestions for Belle II experiment.